DOKUZ EYLÜL UNIVERSITY

GRADUATE SCHOOL OF NATURAL AND APPLIED SCIENCES

PRODUCTION AND CHARACTERIZATION OF METAL ALLOY COATINGS FOR ELECTROMAGNETIC SHIELDING APPLICATIONS

by

Karun Kaan ÖLÇEN

September, 2024

İZMİR

PRODUCTION AND CHARACTERIZATION OF METAL ALLOY COATINGS FOR ELECTROMAGNETIC SHIELDING APPLICATIONS

A Thesis Submitted to the
Graduate School of Natural and Applied Sciences of Dokuz Eylül University
In Partial Fulfillment of the Requirements for Master of Science in
Department of Nanoscience and Nanoengineering, Nanoscience and Nanoengineering Program

by

Karun Kaan ÖLÇEN

September, 2024

İZMİR

M.Sc THESIS EXAMINATION RESULT FORM

We have read the thesis entitled **"PRODUCTION AND CHARACTERIZATION OF METAL ALLOY COATINGS FOR ELECTROMAGNETIC SHIELDING APPLICATIONS"** completed by **KARUN KAAN ÖLÇEN** under supervision of **ASSOC.PROF.DR. TUNCAY DİKİCİ** and we certify that in our opinion it is fully adequate, in scope and in quality, as a thesis for the degree of Master of Science.

Assoc.Prof.Dr. Tuncay DİKİCİ

Supervisor

Assoc.Prof.Dr. Metin YURDDAŞKAL

Jury Member

Assist.Prof.Dr. Hüseyin Erdem YALKIN

Jury Member

Prof. Dr. Okan FISTIKOĞLU

Director

Graduate School of Natural and Applied Sciences

ACKNOWLEDGMENT

I would like to express my gratitude and offer my sincere thanks to my esteemed advisor Assoc. Prof. Dr. Tuncay DİKİCİ and esteemed teacher Assoc. Prof. Dr. Mustafa EROL, who not only helped me with their vast knowledge and unique experiences within the scope of my research and experiments during my master's degree education, including this study, but also always encouraged me to do research with their rational, sincere and caring behavior. I would also like to thank my dear teacher R. A. Zeynep ERTEKİN for her assist from the beginning to the end of my thesis study and for answering all my questions.

I would like to express my gratitude to my valuable teachers, Assoc. Prof. Dr. Sibel OĞUZLAR and Dr. Hilmiye Deniz ERTUĞRUL UYGUN, at Dokuz Eylül University, Electronic Materials Research and Application Center (EMUM), Science and Technology Application and Research Center (TEAM), who helped turn our work into a real thesis study, for providing resources to help me with my experiments and devotedly supporting me in the analysis processes.

I would like to thank my valuable teachers R. A. Özgür Yasin KESKİN, Dr. Sibel Demiroğlu MUSTAFOV and Scientific Researcher Dr. Ulaş BAYSAN, who assisted me when I was in a difficult situation, sometimes in analysis and sometimes in terms of literature knowledge and experience.

I would like to thank my dear friends Erdem Tevfik ÖZDEMİR, Neslihan ŞAKAR, Begüm UZUNBAYIR, Melisa ATAY, Berkay COŞKUN, Sezer BALKAN, Tuna Kaan KAYA and Onur ÇETİNKAYA, who helped me on different issues during this process and with whom we brainstormed during my master's degree.

Finally, I would like to thank my entire family friends, family, especially my mother, sister and father, who supported me with great patience, dedication and self-sacrifice, and who helped me overcome the difficulties I suffered during this long, difficult but also experience-giving process that gave me the happiness of being successful.

Karun Kaan ÖLÇEN

PRODUCTION AND CHARACTERIZATION OF METAL ALLOY COATINGS FOR ELECTROMAGNETIC SHIELDING APPLICATIONS

ABSTRACT

In recent years, the rapid advancement of electronic products and telecommunications has resulted in the issue of electromagnetic interference. This phenomenon, caused by numerous electronic devices like microwave ovens, cell phones, and personal computers, etc.., can lead to data loss, misinterpretation of data, improper operation, and mediocre performance of devices. Additionally, long-term exposure to electromagnetic fields is highlighted as potentially harmful to human health, causing issues such as headaches, eye problems, cancer, and insomnia. The aim of this thesis is to investigate the surface properties of different alloy coatings (Zinc-Nickel, Zinc-Cobalt, Nickel-Cobalt and Zinc-Nickel-Cobalt) and their effects on electromagnetic interference shielding effectiveness. These alloy coatings are electrodeposited onto copper foil surfaces using a sulfate bath and a power supply. The composition, morphology, and phase structures of the coatings are analyzed using Scanning Electron Microscopy, X-ray Diffraction, and X-ray Photoelectron Spectroscopy. Electromagnetic absorption and shielding properties in the X-band frequency range are investigated with a Vector Network Analyzer using coaxial holder method. The surface morphologies of the coatings differed depending on the alloy type. X-ray diffraction reveals distinct phases depending on the alloy type. In the results of the analysis made using the vector network analyzer, results that increased the efficiency of the substrate were obtained in many samples. These binary and ternary metal alloy coatings show promise as effective alternatives to enhance shielding efficiency for materials like copper, which already exhibit good conductivity and some degree of shielding capability.

Keywords: Metal alloy coatings, Surface morphology, Electromagnetic interference shielding, Absorption

ELEKTROMANYETİK KALKANLAMA UYGULAMALARI İÇİN METAL ALAŞIM KAPLAMALARIN ÜRETİMİ VE KARAKTERİZASYONU

ÖZ

Son yıllarda elektronik ürünlerin ve telekomünikasyonların hızla ilerlemesi elektromanyetik girişim sorununa yol açmıştır. Mikrodalga fırınlar, cep telefonları ve kişisel bilgisayarlar gibi çok sayıda elektronik cihazın neden olduğu bu fenomen, veri kaybına, verilerin yanlış yorumlanmasına, uygunsuz çalışmaya ve cihazların vasat performans göstermesine yol açabilir. Ek olarak, elektromanyetik alanlara uzun süreli maruz kalmanın insan sağlığı için potansiyel olarak zararlı olduğu ve baş ağrısı, göz sorunları, kanser ve uykusuzluk gibi sorunlara yol açtığı vurgulanmaktadır. Bu tezin amacı, farklı alaşım kaplamaların (Çinko-Nikel, Çinko-Kobalt, Nikel-Kobalt ve Çinko-Nikel-Kobalt) yüzey özelliklerini ve elektromanyetik girişim kalkanlama etkinliği üzerindeki etkilerini araştırmaktır. Bu alaşım kaplamalar, bir sülfat banyosu ve bir güç kaynağı kullanılarak bakır folyo yüzeylerine elektrokaplanır. Kaplamaların bileşimi, morfolojisi ve faz yapıları, Taramalı Elektron Mikroskobu, X-ışını Kırınımı ve X-ışını Fotoelektron Spektroskopisi kullanılarak analiz edilir. X-bant frekans aralığındaki elektromanyetik emilim ve kalkanlama özellikleri, koaksiyel tutucu yöntemi kullanılarak bir Vektör Ağ Analizörü ile araştırılır. Kaplamaların yüzey morfolojileri alaşım türüne göre farklılık göstermiştir. X-ışını kırınımı alaşım türüne bağlı olarak belirgin fazlar ortaya koymaktadır. Vektör ağ analizörü kullanılarak yapılan analizin sonuçlarında, birçok numunede altlığın verimliliğini artıran sonuçlar elde edilmiştir. Bu ikili ve üçlü metal alaşım kaplamalar, halihazırda iyi iletkenlik ve bir miktar kalkanlama kabiliyeti gösteren bakır gibi malzemeler için kalkanlama verimliliğini artırmak için etkili alternatifler olarak ümit vericidir.

Anahtar kelimeler: Metal alaşım kaplamalar, Yüzey morfolojisi, Elektromanyetik girişim kalkanlama, Absorpsiyon

CONTENTS

Page

LIST OF FIGURES

Page

LIST OF TABLES

Page

CHAPTER ONE
INTRODUCTION

1.1 Background

The use of electronic devices, which emerged in the third phase of the industrial revolution (1969-2010s), has not only brought many innovations and opportunities to almost all companies in terms of production since then, but has also been an important step in solving many problems in daily life and speeding up the functioning of life in general.

The process which initially started with programmable logic controllers, has enabled the schematic creation and subsequent production of new and more functional devices, especially the acceleration of production in factories, as well as the ease on realization of important elements such as data storage, and although it takes time to learn innovations, it has considerably reduced the workload on people.

Of course, all these opportunities and positive features have also brought some negative aspects. The most striking of these is the effects of 'electromagnetic interference' between devices. In the fourth phase of the industrial revolution we are in today (2010s-present), this problem has continued to increase after the development of communication systems that have left their mark on the world and the devices were left to autonomous control.

This phenomenon, caused by various electronic devices for instance mobile phones, tablets, computers, and microwave ovens, can result in data loss, incorrect perception of data, malfunction and substandard performance of many devices.

In addition, it is asserted that long-term exposure to electromagnetic fields is potentially harmful to human health and causes problems such as insomnia, headaches, cancer and eye problems. Various solutions are being sought to prevent electromagnetic interference that causes problems to technological products according to different frequency ranges in each area of the electromagnetic spectrum. In this regard, composite materials, hybrid epoxy materials, nanowire and nanofiber

materials, carbon fiber materials, metal powders, polymer-added films, alloy coatings and many similar products are obtained and used as a result of some experiments.

In a study conducted by Maria in 2014, Cu-Ni ferrite nanoparticles synthesized inside micro-silica particles were made into composite materials together with carbon nanofibers/nanotubes and finally reached a three-dimensional state. Afterwards, electromagnetic interference shielding data in the range of 1-18 GHz were examined (Crespo Ribadeneyra, 2014). Bheema and Etika, synthesized some hybrids and composites including Fe_3O_4, copper nanoparticles (CuMP) and epoxy composites to investigate which material has the better shielding effectiveness across X-band (Bheema and Etika, 2023). A study investigating the X-band electromagnetic interference shielding efficiency of biopolymer aerogels with high flexibility and ultralight, produced by facile freeze-casting method using cellulose nanofibers and silver nanowires was conducted by Zeng et al (Zeng et al., 2020). In 2013, Matthew Ryan Frahm wrote a thesis on using carbon fiber instead of aluminum for electromagnetic shielding in lithium-ion batteries. Carbon fiber with silver paint adhesive, aluminum powders, and aluminum mesh were analyzed between 50 Hz and 25 MHz and their shielding efficiencies were calculated (Frahm, 2013). Copper oxide powder produced using some chemicals was characterized after being silver coated by chemical reactions and the change in electromagnetic shielding efficiency compared to the uncoated state was investigated by Kim et al. with the coaxial transmission line method (Kim et al. 2010). In another study, the electromagnetic shielding amounts of composite polymeric films prepared using solvent casting technique with the help of magnetic nanoparticle modified-graphene nanoplatelet (Fe_3O_4-GNP) and some integrations in polyvinyl alcohol (PVA) matrix were measured using the waveguide method in Ku (12-18 GHz) band & X (8-12 GHz) band and their usability was investigated (Savaş, 2023). In a study on alloy coatings, Ni electroplating and Ni electroless plating were performed on polyacrylonitrile (PAN) based carbon fiber fabrics by varying the coating time and current density. Electromagnetic shielding efficiencies were investigated in three different frequency ranges (İrgin, 2022).

Alloy coatings have the potential to be important and useful in terms of electromagnetic shielding as well as increasing the life of the material because they

provide high corrosion and wear resistance to the substrate material and also have strong electrocatalytic and magnetic properties. Electroplating (Zhang et al., 2021), electroless (autocatalytic) plating (Liu et al., 2010), physical vapor deposition (Li and Sun, 2022), chemical vapor deposition (Ramirez et al., 2023), and plasma spraying techniques (Qing et al., 2021) are used in the production of these materials.

In this study, it is aimed to characterize the products obtained from the applications of binary Zn-Ni, Zn-Co, Ni-Co and ternary Zn-Ni-Co alloy coatings by depositing three different metals (Zn, Ni and Co) on the copper material surface with different combinations by electroplating method. The aim of the study is testing the electromagnetic interference shielding and radar absorption properties of the coatings and to reveal the product with the highest electromagnetic interference shielding efficiency as a result of experiments with different parameters. In the first step on this path, four types of coatings with high wear and corrosion resistance and durability were produced, except for the bath contents and some special differences (alloy coating bath temperature, current densities varying according to the baths). Afterwards, by making changes on the coating parameters (time, current density, double-surface coating), the products with the closest shielding and absorption properties to the desired ones were determined as a result of some characterizations.

1.2 Organization of the Thesis

This thesis consists of eight chapters including this one. As anticipated, chapter one is an introductory covering the aim, motivation and background information of the thesis. Theoretical aspects of pure and alloy coatings and their properties are mentioned in chapter two. Production methods and the factors affecting the alloys are also briefly told in this chapter. Chapter three consists of many essential factors which have numerous effects on coatings, including some pretreatment applications and coating properties in which electrolyte properties are the lead. Chapter four presents a mid-scope analysis on coating production methods and why the electroplating method is chosen for the experiments in this thesis. In chapter five, negative effects of electromagnetic interference and several paths to overcome this phenomenon are discussed in general. Importance of metal alloy coatings assisting for creating a well-

developed substrate having decent electromagnetic interference shielding and further radar absorbing capacities are also mentioned in the chapter. Chapter six consists of the detailed demonstration of experimental studies, indicating the material preparations, applications, testing, characterization with both graphical and theoretical analysis. Chapter seven presents results and discussions whereas conclusions and possible future works are shared in the eighth chapter.

CHAPTER TWO
PURE & ALLOY COATING TYPES AND PROPERTIES

2.1 Coating Types

2.1.1 Pure Coatings

2.1.1.1 Zinc (Zn) Coatings

Zinc element widely used to protect ferrous based materials (e.g. iron, steel, etc...) against corrosion in several industries such as in industrial machines, most spare parts of construction machines (Fig. 2.1), and as underpaint for increasing corrosion resistance in the automotive industry, due to its electrochemical properties and economic suitability (Lodhi et al., 2008).

Figure 2.1 Zinc plating sample

The dissolution rate is constant, therefore the lifetime of zinc coatings is generally directly proportional to their thickness. According to research, it has been determined that a zinc coating of 0.06-0.012 mm is sufficient against rust, and a thickness of 0.024-0.048 mm is sufficient against corrosion in humid or industrial environments (Hasçalık and Özek, 2002). Zinc coatings have physical properties such as good adhesion and

shapeability, and the structural and mechanical properties of the main material do not change. Zinc coating facilities are simpler to install than other coatings. Thus, zinc coating becomes advantageous over others in terms of the costs of the medium prepared for its production. Among hot dipping, electroplating, electroless plating and mechanical coating methods of zinc coating, electroplating is the most preferred one as it has a simple application, and has repeatability. There are three baths used for manufacturing zinc coatings using electrodeposition: acidic, alkaline and cyanide. While acidic zinc coatings have a shiny appearance, coatings obtained from alkaline zinc baths have a more homogeneous coating thickness. Due to this feature, an increase in the use of alkaline zinc baths has been observed in recent years (Çetinkaya, 2006).

2.1.1.2 Nickel (Ni) Coatings

In addition to being a durable and strong material, the fact that it can be used in many areas has made nickel coatings more special and constantly preferred in the industry over the years (Zamani et al., 2016). Functional, decorative and electroforming sections are the three main branches in which nickel electroplating usually classified. Functional applications are which initially comes up to the mind such as enhancing corrosion and wear resistance, amplifying magnetic and other properties. Decorative section is where nickel coatings are generally paired with electroplated chromium in single-layer to obtain a mirror-like brightness. This can be further improved as the thickness (layer amount) is increased, which upgrades the corrosion resistance as well. Lastly, electroforming is where masks or mandrels used as a substrate and nickel is deposited onto them, removed afterwards. After intended shape of nickel electroplating is achieved, it can be used anywhere such as nickel anode materials, quality control (Di Bari et al., 2010), etc... There are three baths used for producing nickel coatings similar to zinc coatings which are sulphate, chloride and sulphamate baths. Although there are several varieties in these methods throughout the years, sulphate (Watts type) baths are commonly used due to their low costs in general (Wang et al., 2013). Some nickel plated parts are shown in Figure 2.2.

Figure 2.2 Ni plating sample

2.1.1.3 Cobalt (Co) Coatings

Due to the high prices of cobalt salts and therefore baths, the fact that cobalt generally precipitates less in combinations such as zinc-cobalt and nickel-cobalt, and that zinc is easier to use, cobalt coatings have rarely been preferred, even though they have similar properties to zinc and nickel coatings. According to the research, cobalt coatings were used instead of nickel coatings for a while in the past, but its frequency of use has declined. It was later used again commercially in printing plates, thanks to its strong reflectivity, high resistance to oxidation and decent hardness. In particular, it is an important factor that it increases the corrosion resistance of nickel coatings and turns them into bright nickel (Soderberg et al., 1941). Although the cost of cobalt is still high today, its applications have increased considerably due to the effects of its alloys with other coatings in decorative and industrial areas.

2.1.2 Alloy Coatings

When it comes to alloy coating, the first thing that comes to mind is the interaction between two or more substances in which they drastically become one material by dissolving in each other in their molten forms. However, as A. Brenner mentioned, this definition is inadequate because it cannot explain such conditions where some metal combinations (e.g. nickel-silver, lead-zinc, etc..) do not form an alloy as they are not soluble in each other. These mixture of metals can be obtained through different methods such as powder metallurgy, and the product still counts as an alloy. Thus, various combinations on different scales can be considered as alloys, even if it is one-phased like copper turnings, in which the copper particles are well diffused in the lead so neither of their individual particles could be identified easily without the help of a microscope (Brenner, 1963).

The chemical composition, phase structure and physical properties of the alloy to be obtained are determined by the electrolysis parameters. These paramaters can be categorized into three main groups; composition of the plating bath (concentration of metal ions to be plated, pH value of the electrolyte, concentrations of complexing agents and chemical additives), operating conditions (type of applied current, current density, temperature and mixing) and the total effect of cell geometry, base material and shape, and coating thickness (Manazoğlu, 2013).

Alloy coatings are preferred in cases where a metal coating requirement requested for testing, analysis, experimentation or use cannot be met with a pure metal (Kanani 2004). Binary zinc-nickel (Zn-Ni), zinc-iron (Zn-Fe) and zinc-cobalt (Zn-Co) coatings show better corrosion resistance than pure zinc. Binary nickel-cobalt (Ni-Co) alloys are preferred for shaping by electrolysis due to their high strength. The corrosion resistance of the ternary zinc-nickel-cobalt (Zn-Ni-Co) alloy is further improved compared to binary alloys (Eliaz et al., 2010). For this reason, the use of such coatings continues to increase, especially in the automotive industry.

Diverse methods are used for manifacturing of metal alloy coatings. Electroplating, pulse plating, composition modulation, electroless (autocatalytic) plating, plasma spraying, physical vapor deposition (PVD) and chemical vapor deposition (CVD)

techniques are the mentioned ones (Eliaz et al., 2010; Zhang et al., 2021; Sekar et al., 2015; Tóth et al., 2013).

Compared to other techniques, electroplating method is simpler to apply, cost-effective and offers repeatability without the need for high temperature and pressure, which has increased its use over time instead of other manufacturing methods (Lupi et al., 2011; Li et al., 2014). The reasons for this are its various advantages, such as adaptability, favorable deposition rate, reasonable costs with the potential to control structure and thickness of deposits even in complex shapes (Karimzadeh et al., 2019).

2.1.2.1 Anomalous Codeposition (ACD)

Abner Brenner is the first to use the term “anomalous codeposition (ACD)” to define a phenomenon that occurs differently than normal during electrochemical deposition process. The situation here is that the less noble metal deposits primarily (higher weight percentage (wt%)) on the target, and it is generally seen in alloy coatings formed by zinc, nickel, cobalt, cadmium, iron, etc.. which are in the transition metal groups (Brenner, 1963; Eliaz et al., 2010).

2.1.2.2 Zn-Ni Coating

Like zinc coatings, its alloy coatings are frequently used in some industries for instance electrical and electronics, automotive, house decoration, aerospace and fasteners industries (Ghaziof and Gao, 2014). Most famous reasons for this phenomenon are that Zn alloys can contribute higher corrosion resistance, thermal stability, mechanical properties compared to pure Zn coatings in a great extent (Bhat and Shet, 2020; Rahman et al., 2009; Tozar and Karahan, 2014; Sriraman et al., 2013). Although cadmium (Cd) and titanium (Ti) were initially preferred as complements of zinc-metal (Zn-M) alloys, over time they were replaced by other metals due to the toxicity of cadmium and the excessive cost of titanium (Ghaziof and Gao 2014; Rahman et al., 2009; Tozar and Karahan, 2014). Common replacements are the iron group of transition metals which are nickel (Ni), cobalt (Co) and iron (Fe) (Ghaziof and Gao, 2014; Bhat and Shet, 2020; Rahman et al., 2009; Tozar and Karahan, 2014; Sriraman et al., 2013; Panek et al., 2010; Elkhatabi et al, 1999). Zinc-nickel (Zn-Ni)

alloy coatings (Fig. 2.3) were the beginning of the new era of Zn-based coatings because pure Ni plating was more well-known than pure Co plating at the time.

Figure 2.3 Zn-Ni plating sample

Shortly after Zn-Ni coatings began to be used, they easily attracted attention thanks to their known advantages (enhanced corrosion resistance, better mechanical properties in general) compared to pure Zn coatings (Ghaziof and Gao, 2014). Zn element is the one that deposits the most in terms of wt% due to the process being an anomalous codeposition as mentioned before, in which the less noble metal is higher in wt% (Eliaz et al., 2010; Ghaziof and Gao, 2014). Sometimes there can be more than one phase in the coatings, depending on the wt% in the coatings. According to many research, the deposits where Ni content in the 8-14 wt% interval with single phase are considered the best result in terms of corrosion resistance, which is five times better than pure Zn (Ghaziof and Gao, 2014; Tozar and Karahan, 2014).

2.1.2.3 Zn-Co Coating

Zinc-cobalt (Zn-Co) coatings (Fig. 2.4) are also a popular choice among other Zn-M alloys due to the resemblances between Zn-Co and Zn-Ni alloy coatings, even if the required wt% changes according to respective element. Just like Zn-Ni coatings, Zn-Co coatings have enhanced corrosion resistance and mechanical properties than pure versions of individual elements. They also scored positive on the salt spray test, meaning that they passed the test with no whisker growth (Karahan et al., 2009).

Figure 2.4 Zn-Co plating sample

Although there are many similarities, there are some signature features that seperates both coatings, which magnificent brightness of Zn-Co alloys is one of them (Bhat and Shet, 2020). Therefore, most of the characteristics are suitable for applications in various industries such as electrical and electronics, automotive industry, fasteners industry (Bhat and Shet, 2020; Karahan et al., 2009; Mahieu et al., 1999), etc… The levels of good properties of Zn-Co alloys vary considerably depending on the percentage of cobalt in them, as in Zn-Ni alloys. However, more than

1 wt% Co is sufficient to surpass the effect of pure zinc alloys (Lima-Neto et al., 2007). Since the deposits of all the previously mentioned alloys consist in the form of anomalous codeposition (Eliaz et al., 2010; Ghaziof and Gao, 2014), it is correct to evaluate on the cobalt ratios when investigating the properties of zinc-cobalt coating. Although, at first glance, it was thought that zinc-cobalt alloys containing 1% cobalt gave the best efficiency as a result of the experiments and research carried out (Kalantary, 1994), subsequent additional research showed that good efficiency could also be obtained at higher rates. The reason of this phenomenon is most likely related to the single phase – more than one phase situation of Zn-Co coatings according to Co wt%, which is similar to the Ni wt% that of Zn-Ni coatings. Lodhi et al.'s studies show that coatings with high cobalt content (15-30%) show better corrosion resistance in general (Lodhi et al., 2008).

2.1.2.4 Ni-Co Coating

Ni-Co alloys are one of the coating types that gained popularity in recent years, after the investigation of the effects of individual elements in Zn-based coatings. Similar to previous coatings, Ni-Co coatings (Fig. 2.5) are upgraded coatings in terms of properties such as high strength, decent wear resistance, high toughness, suitable electrocatalitic activity and advanced corrosion resistance (Zamani et al., 2016; Zhang et al., 2021; Karimzadeh et al., 2019; Yang et al., 2011; Tian et al., 2011).

Figure 2.5 Ni-Co plating sample

In addition to these features, the fact that they can be used decoratively has also increased the interest in them (Karimzadeh et al., 2019; Tian et al., 2011). What really makes Ni-Co coatings stand out from other binary coatings and enables them to open up to different applications are their special magnetic properties (Karimzadeh et al., 2019; Yang et al., 2011). This situation assists the use of Ni-Co coatings in electronics and computers. Memory cards, drums, discs, microelectromechanical systems (MEMS), shape memory alloys, soft magnetic films, tapes are common examples (Karimzadeh et al., 2019, Zhang et al., 2021; Tian et al., 2011). As mentioned above, Ni-Co alloys are produced through ACD, when the less noble metal primarily deposits (Eliaz et al., 2010; Ghaziof and Gao, 2014), which nickel is the one that precipitates in this situation. Therefore, adjusting cobalt content aids to better understanding of how the so called properties of Ni-Co alloy coatings change. According to some research, physicochemical properties, structures and even magnetic properties are all affected by Co content (Karimzadeh et al., 2019, Zhang et al., 2021; Tian et al., 2011).

2.1.2.5 Zn-Ni-Co Coating

Zn-Ni-Fe ternary alloys are either studied as the main alloy or assists for comparing some binary metal alloy + non-metal composites. However, Zn-Ni-Co ternary alloys are slowly beginning to be preferred as an alternative as some important aspects of Ni-Co alloys are more likely to known nowadays. Now that all binary combinations (Zn-Ni, Zn-Co and Ni-Co) have been inspected, ternary Zn-Ni-Co alloys are produced to improve the general features of these coatings, anti-corrosion properties being in the first place (Bhat and Shet, 2020).

2.2 Coating Parameters

2.2.1 Coating Thickness

According to the electrolysis law discovered by Michael Faraday, there is a directly proportional connection between the current passing through the electrolyte and the ions transferred to the substrate, thus increasing the current passing through the solution technically makes the coating thicker. In this context, the thickness of the coating can be brought to the desired value by altering the current density and therefore the deposition time. As reported by Faraday to deposit 1 gram equivalent of a metal, 26.799 ampere-hours or 96.500 coulombs (ampere-seconds) amount of electricity is needed, which is known as Faraday's Constant. He also specifies the connection between the number of electrons involved and valency of the metal, called the ratio of atomic weight to valence electrons the "equivalent weight" or "chemical equivalent" of the metal. Using this constant, atomic weight and valence electron number of any element, total deposited metal amount can be found. For instance, Weight of Ni ($\boldsymbol{W_{Ni}}$) can be written as:

$$W_{\mathrm{Ni}} = x * I * t \tag{2.1}$$

$\boldsymbol{W_{Ni}}$ represents the quantity of Ni deposited at the cathode in grams, while $\boldsymbol{I}$ denotes the current passing through the plating bath in amperes, and $\boldsymbol{t}$ represents the duration of current flow in hours. As atomic weight of Ni is 58.70 g and valency is 2 which makes the equivalent weight 29.35 g, the equation turns into following:

$$29.35\ g = x * 26.799\ Ah \tag{2.2}$$

$$\rightarrow x = 1.095\,\frac{g}{Ah}$$

Therefore;

$$W_{\mathrm{Ni}} = 1.095 * I * t \tag{2.3}$$

Which means if the current efficiency is 100%, 1.095 grams of Ni will be deposited in 1 ampere-hour. When it comes to implementation, the results are not like this usually because of some other electrochemical reactions, which decreases the current efficiency. For this reason, cathode current efficiency, as its full name, may decrease to different percentages depending on which element is used. According to Nickel Handbook of Nickel Institute, the cathode current efficiency of nickel depositions often taken as 95.5% in calculations. Using $\boldsymbol{W_{Ni}}$, density of Ni (8.907 $g.cm^{-3}$), and the surface area to be coated (***A***, in dm^2), average coating thickness (ACT) can be calculated:

$$ACT_{\mathrm{Ni}} = \frac{1.095 * I * t}{8.907 * A} * 100 \tag{2.4}$$

When all the data is collected in one, the equations can be generalized as:

$$W_{\mathrm{m}} = n * I * t \tag{2.5}$$

$$ACT_{\mathrm{m}} = \frac{W\mathrm{m}}{p * A} * 100 \tag{2.6}$$

Where ***m*** represents the metal element used in plating, ***n*** is the factor of how many grams of the used element will be deposited in 1 ampere-hour and ***p*** indicates the density of the metal element (Rose and Whittington, 2022).

2.2.2 Coating Structure

Using different production methods also creates differences in coating structures. Manipulating the microstructure of materials cost-effectively facilitates the creation of innovative high-performance materials. This can be attained through simple, budget-

friendly techniques suitable for industrial applications, e.g. electrodeposition (Aliofkhazraei et al., 2021). The nature of the interface between the base metal and the coating reflects the strength of their bond. A clear boundary suggests that the primary bonding mechanism between the coating and the base metal is mechanical interaction. In this scenario, it is essential for the coating to closely adhere to the metal surface, replicating its texture. Disruptions at the interface indicate a poor quality deposition process (Tushinsky, 2002).

2.2.3 Coating Morphology

The use of various current control modes also affects the microstructural properties and morphology of the deposits, similar to the effect of the chemical composition of the plating bath. Pulsed current, for instance, affects mass and charge transfer during coating, while reverse anodic current may enhance structural and mechanical properties. In direct current (DC) electrodeposition, adjustments in deposition time and current density lead to multilayer coatings. However, with pulsed current, additional parameters like frequency, duty cycle also play a role in the process (Aliofkhazraei et al., 2021).

2.2.4 Coating Surface Roughness

Commonly employed surface roughness parameters include the mean deviation from the average height and peak density. However, various other parameters such as surface area, angularity, and sharpness are also significant in surface analysis. Coatings must meet strict appearance criteria. For instance, automotive coatings often need to be highly glossy and thin to be cost-effective and lightweight, requiring a smooth surface without pronounced profiles underneath. In such cases and others alike, a chemical conversion of the surface is employed to prevent corrosion and enhance adhesion, maintaining a surface roughness significantly smaller than the coating's thickness. The thickness of a coating is typically determined by its intended purpose. For instance, if a coating is meant to serve as a barrier against water and corrosive substances, it should be sufficiently thick to offer protection throughout its expected lifespan. If a coating needs to withstand mechanical stresses, such as when it's buried in infrastructure, a thicker coating will provide greater resilience. Because metals

generally exhibit greater strength and toughness compared to organic coatings, it is advantageous for the structural strength of the composite if metal protrusions penetrate deeply into the coating thickness. A coating with a thickness of approximately 1000 μm can be applied over a surface profile that extends to several hundred micrometers in height. However, economic factors may impose limitations on the maximum thickness of the coating that can be applied (Croll, 2020).

2.2.5 Mechanical Properties

Various methods have been proposed to improve material properties for specific purposes, including heat treatment, alloying, and coatings. Coating processes, in particular, offer significant material enhancement as they can reduce costs and ease material insufficiency since coating layers are typically only micrometers thick. This means less material is required to create coating layers on a substrate. Coatings can provide a range of properties such as thermal insulation, altered surface texture, corrosion and wear resistance, electrical insulation, increased surface hardness, improved wettability, hydrophobicity, and more. There are numerous coating methods available due to diverse applications across different fields, each with its set of online and offline parameters leading to varied outcomes in terms of microstructure, effectiveness, suitability, and durability. However, coating methods are particularly beneficial in applications where corrosion and wear protection are critical. Corrosion can compromise the mechanical properties of materials, and the release of corrosion products may lead to a more aggressive corrosive environment or unwanted effects in multiple applications (Fotovvati et al., 2019).

2.2.6 Corrosion Properties

Corrosion is essentially the interaction between metal and its environment, resulting in alterations to the metal's properties and potentially affecting its role within a system or medium. When external environmental factors begin to impact the material's integrity, it becomes necessary to shield it from these adverse effects. One of the important points is that coatings are good corrosion inhibitors. Therefore, it can be said that almost every coating, including those used commercially, has good anti-corrosive properties. Introducing coatings stands out as the optimal solution for safeguarding

metallic surfaces. As corrosion is an undesirable occurrence that one aims to prevent, it is a phenomenon that must be fully understood in order to mitigate its effects (Nazeer and Madkour, 2018).

CHAPTER THREE
FACTORS EFFECTING THE QUALITY OF THE COATING

3.1 Coating Pretreatment Applications

3.1.1 Acidic Cleaning

Acidic cleaning is the process of removing residues such as rust and dirt on the surface of the part before coating. The cleaning process is carried out in an acidic environment (acid baths consisting of 20-50 % acid) to carefully and meticulously remove these deposits from the surface, which are commonly encountered on the surfaces of iron, steel and similar metals. The samples are immersed in these prepared dilute acidic liquids and the residues on the surface are removed. However, in order for this process not to harm the substrate surface, it is necessary to take some precautions, such as the use of inhibitors, to prevent the part surface from corroding after deposits on the surface. Diluted hydrochloric acid (HCl) and sulfuric acid (H_2SO_4) solutions are the main acids used for this process (Çetinkaya, 2006).

3.1.2 Alkaline Cleaning

Alkaline cleaners are specially formulated proprietary chemical mixtures that include alkaline salts, wetting agents, and chelating agents. These blends, typically containing caustic substances, phosphates, and silicates, along with a equitable amount of surface-active agents, are highly effective for cleaning metals. When dissolved in hot water and doused on dirty surfaces, these cleaners generally remove most types of soil. This method is both the most cost-effective and efficient for automated cleaning (Sparks, 2008).

3.1.3 Mechanical Cleaning of the Sample Surface

If the roughness level of the sample surface is not as desired before coating, surface polishing is applied. In this process, the surface is wet sanded mechanically with various sandpapers. Then, polishing is done in the polishing machine (Güney, 2020).

3.1.4 Degreasing

Samples may have certain impurities before the coating process. In order to clean the oil and oxide layer, if any, it must be treated with acids and alkalines (Güney, 2020).

3.1.5 Rinsing

Rinsing between baths must be done well, otherwise the baths will become contaminated during transportation. The most effective rinse is done with pure and constantly flowing water. In this case, the used water is thrown away and the washing water remains fresh. This prevents chemicals from being carried to the next bath.

3.2 Coating Properties

3.2.1 Anode & Cathode State

In the plating bath, the cathode is the material on which the coating is made, which is connected to the negative part of the circuit. The anode, which is the coated material, is the electrode connected to the positive part of the circuit. It is always necessary to pre-treat the cathode before plating. Before coating a metal surface, it must be cleaned not only from oil and dirt, but also from other layers on the surface. The first step is to remove grease and dirt using an organic solvent. The sample is then washed completely with water and contacted with an alkaline solution to complete the cleaning. Immersion in acid removes any oxide layer formed during alkali washing and creates a suitable surface for coating. In the plating process, the soluble type of the metal to be coated is used as the anode. In this way, the metal ion concentration is constantly kept constant. Maintaining a constant metal ion concentration in the electrolyte depends on the current efficiency at the anode being the same as that at the cathode. If there is a difference, correction of the concentration should be made at regular intervals. Otherwise, the anode becomes passive and this is a situation that must be prevented (Çetinkaya, 2006).

3.2.2 Electrolyte (Plating Bath) Properties

The electrolyte is an aqueous solution containing the metal to be coated on the sample in ionic form. It is advantageous to keep the metals in an ionic state so that the coating can be done more easily during the process. Therefore, solutions of simple salts of the desired metal are used as electrolytes (Çetinkaya, 2006).

3.2.2.1 Conductivity

A conducting solution in an ionic state in which current is carried by cations and anions which move through opposite directions is called an electrolyte (plating bath). Therefore, the important aspect of electrolytes is the large amount of ions or charged species attracted towards the electrodes. Ions surrounding an electrode are repelled or attracted by the electrode, depending on the charge carried by the ion and the polarity of the electrode. Since metal alloy coatings are produced using electroplating technique, inspecting electroplating electrolytes is important.

It is essential that the electroplating solution, which is an instant source of the metal to be deposited, not only provides the metal but also meets other requirements such as anode dissolution, pH stability, conductivity, etc... High efficiency and low toxicity, that is, minimum consumption of electrical energy per kilogram of deposited metal, are among the features that increase the importance of modern electrolytes. While metal accumulates with 100% efficiency at the rate of one atom per electron, 100% efficient dissolution in a soluble anode and maintenance of metal concentration in solution can only occur in an ideal electrolyte. The solvent of a metal plating bath (electrolyte) is water. The electrolyte contains metal ions to be coated, salts that provide conductivity, and salts that complex with the metal to be coated. Sometimes salts that provide conductivity can also form complexes with metal. Although the resulting metal complexes stand out as a good metal source thanks to their high solubility properties, it is very difficult to provide even low amounts of metal ions due to their extreme stability. Therefore, the 'activity' of metal ions remains extremely low, even in solutions with high metal concentrations. This has the effect of reducing the deposition potential as much as possible to prevent flooding of the substrate metal (Çetinkaya, 2006; Hulse, 1993).

3.2.2.2 Current Density of the Electrolyte

Knowing the current density is very important because it affects the amount and characteristics of the coating on the cathode. The amperage applied per square decimeter (A/dm²) during coating is expressed as current density and can be calculated through following equation:

$$J = \frac{I}{A} \tag{3.1}$$

Where J is the current density (A/dm²), I is the applied current (A), and A is the total area (dm²). In coating, calculations are made by surface area. If it is assumed that the current applied to one of two equal parts with the same surface area is twice the current applied to the other, then the surface of the part with the higher applied current value will be coated with twice as much metal as the other surface. Current density, which gives the amount of electricity applied per second to a unit area, is the most appropriate way to define the magnitude of the current used in the coating (Dikici, 2009).

In the electroplating process, the limit current density is a high value at which the desired coating thickness cannot be achieved. Deposition above this value will have a spongy and powdery appearance. The limit current density value varies depending on the concentration of metal ions in the coating and cell conditions. High concentrations are required for rapid coating (Güney, 2020).

In many coating systems, the cathode current density is in 1-10 A/dm² interval. In order for the deposition thickness to be the same in every region of the surface, the current density must be the same at all points of the cathode. This situation is only possible if the distance between the closest point of the anode and every point of the cathode is the same. In practice, the situation is different; The resistance related to the current between different points of the anode and cathode is different, so the current density at these points is also different. In such cases, the density of deposition is not the same at every point (Koehler, 1944; Çetinkaya, 2006).

When the current density exceeds a certain level, the metal ions discharged near the cathode cannot be adequately met by those coming from the solution, resulting in the deposition at the cathode being less than desired. As a result, the quality of the deposit is poor, that is, a burnt and spongy coating is obtained (Güney, 2020).

3.2.2.3 pH of the Electrolyte

All solutions obtained by dissolving compounds in water contain some hydrogen ions. Because water consists of two hydrogen and one oxygen atom. Considering hydrogen is so tightly bonded to oxygen, the forces that cause ionization have little effect. For this reason, pure water contains very few free hydrogen ions. For example, there is 1 gram of hydrogen ion in 10 thousand liters of water. This is why pure water is a poor conductor. Acids ionize easily and large numbers of hydrogen ions dissolve in water (Dikici, 2009). Coating electrolytes are divided into three: acid, neutral and basic. If the pH of the bath used is low, gas accumulation may occur on the cathode surface as it facilitates gas release (Kavak, 2001; Güney, 2020). In some plating baths, pH value is of great importance. If simple metal salts are used, the solution must be acidic, otherwise the coating metal will precipitate as hydroxide in alkaline solution (Çetinkaya, 2006). Another priority of pH in this work is that the pH value is essential as all metal alloys considered in this thesis deposits with anomalous codeposition. If the pH value on the cathode surface is below the level needed for hydroxide formation, the adsorption of the active (more noble) metal, mono-hydroxides, or metal hydroxides leads to codeposition (Karimzadeh et al., 2019).

3.2.2.4 Electrolyte Composition

The simplest way to have a metal in an ionic state in the electrolyte is to use a solution of a simple salt of that metal. In practice, the main thing that is desired from an economic perspective is the speed of deposition which means high current density. To reduce the effect of concentration polarization at the cathode, the metal ion concentration in the solution must be high. At the same time, in order to provide good conductivity to the solution and reduce resistive losses, the total ionic concentration in the solution must be high. This limits the use of high solubility metal salts. Another limiting factor in metal salt selection is that the metal salt anion does not leave its

charge at the anode. Nitrate, chloride and sulfate are the anions usually used, and mixtures of their salts are also used. The best coating occurs in the electrolyte where the metal salt and other components are present (Çetinkaya, 2006). Although it is easier to adjust the metal content when working with pure metal coatings, it is important to get the setting right when it comes to metal alloy coatings. Because the concentrations at which each metal duo or trio will combine are different. For instance, when we look at the metal alloys made of Ni and Co, we see that they form compounds with many concentration values. This situation offers the researcher the opportunity to work with them in a wide range (Karimzadeh et al., 2019).

3.2.2.5 Bath Temperature

The temperature of the electrolyte bath may vary depending on the structure desired to be obtained. In the coating process, certain operating temperatures are selected according to different bath types. During the alloy coating production in this study, all baths, except the electrolyte bath in which the Zn-Ni alloy was produced, were carried out at 25 °C. During Zn-Ni production, the temperature of the electrolyte bath was set at 60 °C. Hot baths are generally preferred in industry because the solubility and conductivity of metal salts increase in hot solutions. For instance, bright copper and nickel plating baths are carried out at 60-70 °C and the parts are moved. Coatings applied in hot and active baths have higher adhesion strength and better appearance (Güney, 2020).

3.2.2.6 Coating Time

When considered within the scope of Faraday's rule, as the coating time increases, the thickness of the deposit and therefore the corrosion and wear resistance will increase. As in every case, there may be exceptions here too. For example, since the less noble element accumulates more during the abnormal deposition mentioned earlier in the study, the prolongation of the coating process time may bring the element ratio in the alloy to a different point than desired, which will change the phases that will occur in the structure. It can also affect corrosion, wear resistances, mechanical strength, hardness, thickness, morphology and structure of the deposit. Due to these

reasons, controlling coating time is an important issue (Ashassi-Sorkhabi and Rafizadeh, 2004).

3.2.2.7 Stirring Speed

Some of the coating solutions are fixed, some are mobile, so they generally need to be mixed. As a result of the mixing process, the composition of the solution is the same everywhere and this makes it possible to operate the bath at higher current densities. It would be useful to move the sample to be coated in the bath and filter the bath in places to compensate for the local depletion at the cathode. Mechanical and magnetic stirrers are also used to animate the plating baths. The movement of the electrolyte is achieved mechanically by oscillating and rotating a suitable propeller inside the bath. Magnetic mixing can also be done with a magnetizing propeller placed at the bottom of the coating tank. The most practical method of mixing in small-volume coating processes is fish placed in a beaker used on stirrers with magnetic heaters. When the mixer is turned on, the fish in the container filled with solution rotates and performs the mixing process (Güney, 2020).

CHAPTER FOUR
SURFACE COATING TECHNIQUES

4.1 Electroplating (Electrochemical Deposition/Electrodeposition)

Electroplating is the process of depositing metal onto a material surface within a chemical environment through the application of electrical energy. Besides the dissolved metal salt or compound with electrical conductivity in the specified environment, the process involves the utilization of two electrodes known as the anode and cathode to transfer electrical energy to the solution. Usually, the anode in the electrolytic cell consists of the material being deposited and is captivated during the deposition process. However, there are instances where the anode material remains intact, and the material for deposition solely originates from the solution, necessitating continuous replenishment. Figure 4.1 is a demonstration of a sample Zn electroplating circuit including a power supply, a cathode, an anode and an electrolyte.

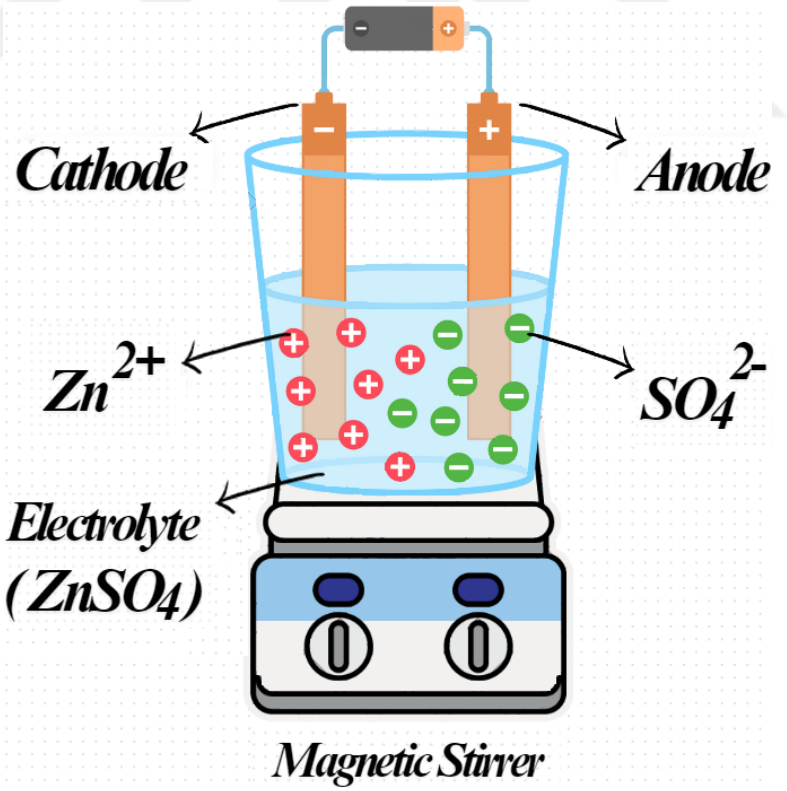

Figure 4.1 Zn electroplating experimental setup

The processes occurring in the circuit can be titled as cathodic and anodic:

Anodic processes:

$½\ O_2 + 2H^+ + 2e- \rightarrow H_2O$

$½\ O_2 + H_2O + 2e- \rightarrow 2OH-$

Cathodic processes:

$Me^{z+} + ze- \rightarrow Me$

$2H^+ + 2e- \rightarrow H_2$

where Me^{z+} is the metallic ion to be coated on the substrate and Me is the coated metal, which is Zn in this case, thus $Zn^{2+} + 2e- \rightarrow Zn$ is the reaction equation (de Carli, 2022).

Electrochemical deposition is an adaptable and cost-effective technique for producing a diverse range of two and three-dimensional materials, including films and coatings. The process relies on electrochemical phenomena associated with the reduction or deposition of electroactive species and other accompanying elements on the cathode surface. Considering these electrochemical principles enhances the controllability of the electrodeposition process for specific purposes and applications (Dikici, 2009; Mattox, 2010; Nasirpouri et al., 2020).

4.1.1 Pulse Plating

Pulse plating is one of the efficient techniques for metal and alloy deposition on surfaces and it is a subtype of direct current (DC) electrodeposition. The main aspect that seperates this method from traditional DC electrodeposition is that there are three variables instead of just current density. These are current ‘on’ and current ‘off’ time, and peak current density. A pulse cycle is formed by alternating on and off times. The subtype simple square wave pulses are the method used for coating applications. Average current density is calculated via following equations:

$$\text{Average current density} = \text{on } time * duty\ cycle \tag{4.1}$$

$$\text{Duty cycle} = \frac{on\ time}{on\ time + off\ time} * 100 \tag{4.2}$$

On-off times vary from microseconds to milliseconds whereas duty cycles from 1 to 100%. Thus, there are limitless combinations of pulse current densities in order to obtain average current density (Devaraj et al., 1990).

4.2 Electroless Plating (Autocatalytic Plating)

Theoretically, Brenner and Riddell have created a coating technique that does not require an external source of electric current to apply coatings on metallic surfaces. Metallic ions, reductants, ligands and some other minor components are present in the complex electrolyte solution which is also the electroplating bath. The chemical reduction of agents catalyzed by often boron (B) and phosphorus (P) is the source of voltage/current in this method. Since the reduction reaction is catalyzed, the technique is also called autocatalytic plating. Electroless plating is generally used for manufacturing electronic parts in industries (Mattox, 2010; Mallory and Hadju, 1990; Ohno, 1991).

4.3 Chemical Vapor Deposition (CVD)

CVD stands as a extensively adopted technology in material processing, predominantly for applying high-quality solid thin-film coatings onto surfaces. Yet, its applications extend to manufacturing high purity powders, bulk materials, and crafting composite materials through infiltration techniques. This versatile method has been employed for depositing a broad array of materials. In its simplest form, CVD involves introducing precursor gas or gases into a chamber with one or more heated substances to be coated. Chemical reactions take place on and around the heated surfaces, leading to the deposition of a thin film surface (Creighton and Ho, 2001; Sun et al., 2021).

4.4 Physical Vapor Deposition (PVD)

PVD processes involve atomistic deposition, where material is vaporized from a liquid or solid source into atoms or even molecules. These particles are then carried in vapor form through a vacuum or low-pressure gaseous or plasma environment to the substrate, where they condense. Commonly, the thickness of deposited films are in between a few to thousands of nanometers. However, they might also be employed to

create multilayer coatings, ultra thick deposits, graded composition deposits, and free-standing structures. Being capable of depositing films of elements, alloys, and compounds using reactive deposition methods demonstrates how versatile PVD processes are (Mattox, 2010).

4.5 Plasma Spraying

Plasma spraying technique is used to melt some of the energy restrained in thermally ionized gases, as in oxyacetylene flame spray, and then push fine powder particles onto a surface so that they agglomerate and adhere to produce a coating. In this way, not only can coatings that increase the lifespan of important components exposed to aggressive atmospheres be created, but also realistic shapes of some complex materials can be produced. For metallic coatings, the high amount of oxide in the residues causes air plasma spraying to be ignored. The most well-known and applied plasma processes are chamber spraying and argon shrouded plasma spraying. Although it has been thought for many years that the experience and individual skill of the operators in the plasma spraying process are very effective during the process, recent research has revealed many other factors that affect the quality of the resulting coating. Some of these have been determined as heat and momentum transfer of flame particles, power of plasma, gas in plasma, particle structure and interfacial bonding (Gill and Tucker, 1986; Suryanarayanan, 1993).

4.6 Composition Modulation

Composition modulation by electrodeposition technique is first tried by Brenner where he used two baths for each component and periodic transfer of the accumulated parts, however, the method cannot be used practically due to its inconvenient usage. Therefore, a single bath deposition for both components' salts included is more reassuring, nevertheless, unfortunately cannot prevent a basic problem about the deposit of the mixed solution. Although it is possible to deposit a layer of the more noble component by maintaining the potential difference between the reduction potentials of the two components, when the potential is adjusted to reduce the less noble component, both metals are anticipated to deposit simultaneously, forming an alloy layer rather than pure metal. As a result of some studies, it has been observed

that modulated alloy coatings produced by this method with a thickness of approximately 1-5 nm are more efficient and have unique properties (Yahalom and Zadok, 1987).

4.7 Sol-Gel Coating

The sol-gel process, originally developed in the 1900s for synthesizing inorganic materials like glasses and ceramics, is now used for coating applications as well (Wu et al., 2020). The process involves converting a precursor solution into a gel through solvent evaporation, followed by curing or sintering to create the needed product. This method is versatile, capable of synthesizing various materials like bulk glass objects, thin films, powders, and fibers. In industrial settings, the focus is on using the sol-gel process for functional and protective coatings. This process can modify surface properties while maintaining the integrity of the bulk material. Due to its simplicity and affordability in terms of equipment, this technique is comparable to surface engineering methods like physical and chemical vapor deposition. By adjusting the method of sol preparation, synthesis parameters, and thermal treatment for sintering and/or consolidation, a diverse array of plating compositions and properties can be attained. Choosing the right coating method and deposition parameters allows for the utilization of various shapes and surfaces, each with unique attributes such as reactivity, hydrophilicity, and roughness (Durán et al., 2007).

CHAPTER FIVE
ELECTROMAGNETIC SHIELDING & RADAR ABSORBING

5.1 Electromagnetic Interference

Electromagnetic interference, which occurs due to the excessive usage of man-made electrical and electronic devices such as microwave ovens, radar systems, computers, cell phones, telecommunication systems, photocopiers, televisions, etc., not only lead to serious malfunctioning on many products which may emerge as data misinterpretation and loss, weak performance but also formidable health issues including eye cancer, insomnia, headaches, migraine. A wide range of applications are conducted to mitigate or eliminate the impact of electromagnetic interference. Several studies on surface treatments have been conducted to develop shielding solutions against electromagnetic waves, utilizing materials like EMI shielding screens, screen coatings, flexible conductor screens, shielding textiles, and broadband microwave absorbers (Araz, 2018). Surface coatings are among the fundamental materials used for efficient electromagnetic interference shielding. In terms of suppressing and negating EMI, absorbers involving ferrite are commonly used because of their high conductivity and complex intrinsic parameters (σ, ϵ, and μ) are well-suited for this assignment. Shielding Effectiveness (SE) is one of the essential parameters of absorber materials in order to characterize them among each other (Araz, 2018; Ye et al., 2015). Electromagnetic waves have been found to affect materials in basically three ways. When it first encounters the shield surface, the energy of the incident wave is attenuated by processes such as reflection, absorption and multiple reflection.

5.1.1 Electromagnetic Interference Shielding

The mean values of shielding are expressed as follows: reflection (SE_R), absorption (SE_A) and multiple reflections (SE_M). An electromagnetic wave can be reflected if and only if there is a huge impedance difference between the propagating medium and the material. Hence, the idea that materials that are good conductors can exhibit high electromagnetic reflectivity is common in the literature. In general, the electromagnetic shielding effectiveness of the material depends on how high its electrical conductivity is or is not, and this is frequently mentioned in the literature.

Since both the specimens and the substrate have high conductivity, no electromagnetic shielding problem is expected in this study. When there are magnetic dipoles within the material, absorption takes place. Multiple reflections might occur upon wave interaction with a surface of a material (Iqbal et al., 2023). A magnetic field (H) and an electric field (E) are the two components of any electromagnetic wave which are perpendicular to each other (Fig. 5.1).

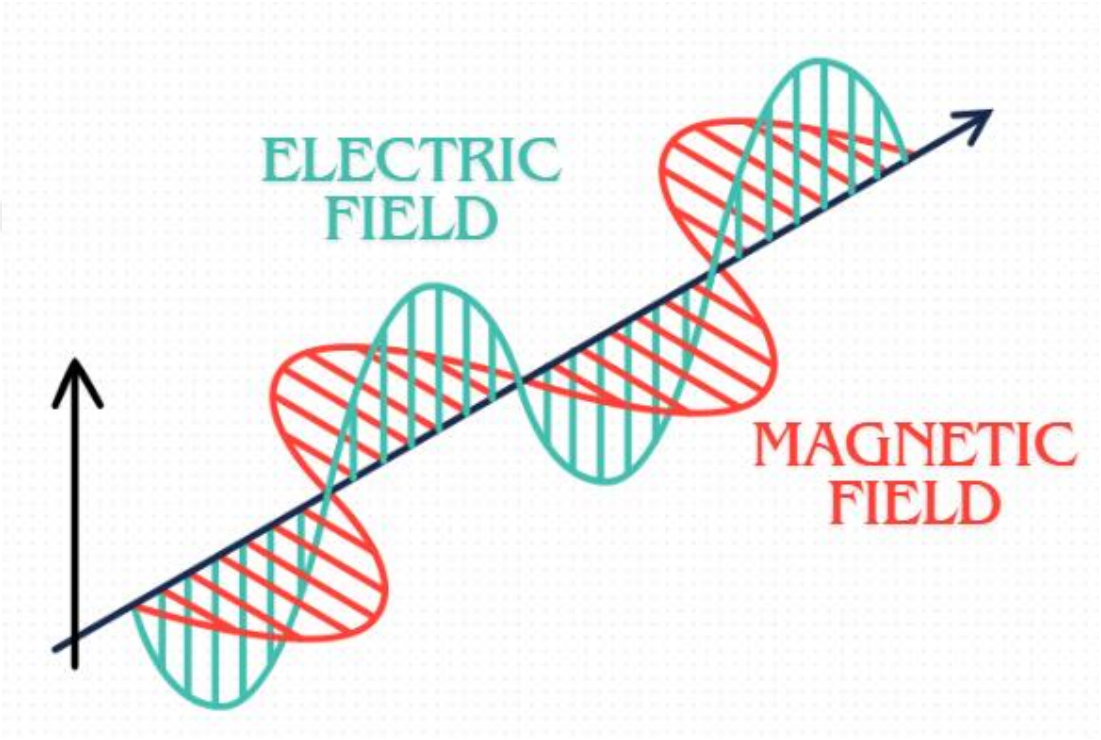

Figure 5.1 Magnetic and electric field distribution of an electromagnetic wave

The relative magnitude depends on the waveform and its origin. The E/H ratio is a description of the wave impedance. EMI shielding originates from t: the far-field shielding region and the near-field shielding region. SE represents the ratio of the field before and after attenuation of the material exposed to the magnetic and electric field and can be formulated as follows:

$$\mathrm{SE} = 20 \log\left(\frac{Et}{Ei}\right) \tag{5.1}$$

$$\mathrm{SE} = 20 \log\left(\frac{Ht}{Hi}\right) \tag{5.2}$$

where E, H, t, and i are electric field, magnetic field, transmitted wave and incident wave respectively.

H is measured in amperes per meter (A/m) whereas E is measured in volts per meter (V/m). SE varies with frequency. Electromagnetic wave attenuation occurs through three forms illustrated in Fig. 5.2: reflection (R), absorption (A), and multiple reflections (M). Therefore, shielding effectiveness is the sum of these three terms:

$$SE = R + A + M \tag{5.3}$$

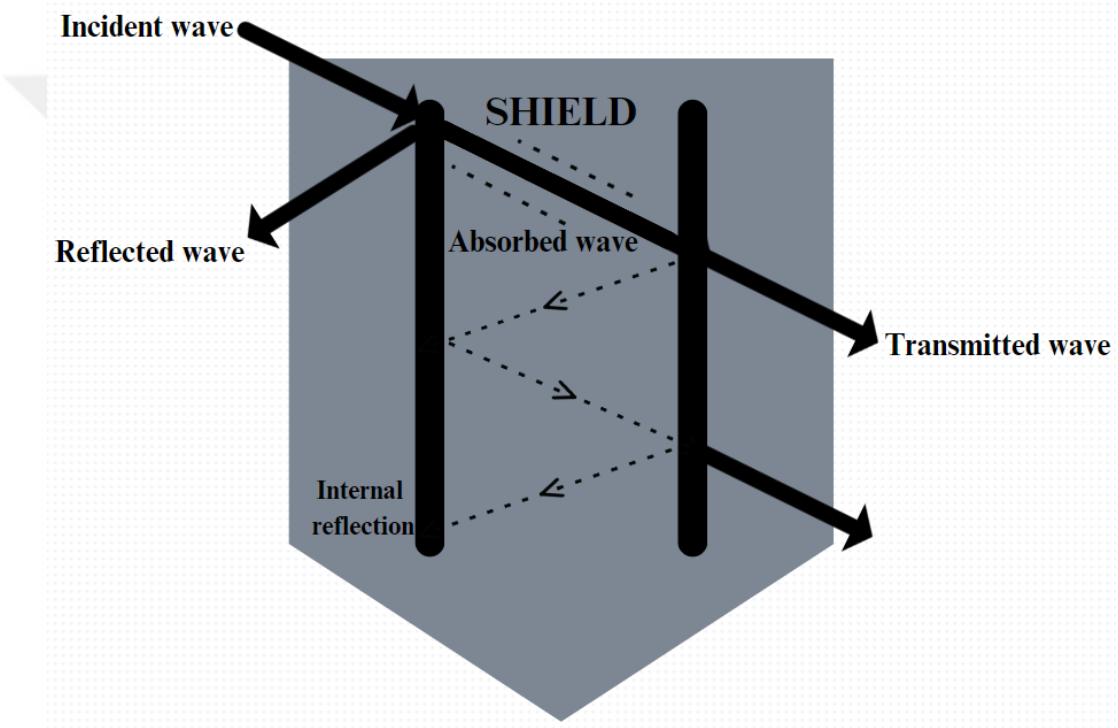

Figure 5.2 Behaviour of the electromagnetic waves attenuated by shielding

Shielded box, free space (open field), coaxial transmission line, and shielded room are the four frequently used test methods for measuring EMI shielding effectiveness (EMI-SE) of a shielding substrate. In this paper, the coaxial transmission line method was preferred for shielding applications due to the suitable environment and available equipment. Initially the shielded box is the most common of the four methods, however, as the coaxial transmission line exceeds the limits of the previous one, it became the preferred approach. Greatest benefit of this method is the comparability of the results regardless of the laboratory where the experiment is performed. Moreover,

this method can be utilized to separate the data into absorbed, transmitted, and reflected components. There are several modes of the device, and the spectrum analyzer mode is the generally used one which demonstrates the system response faster than the others (Geetha et al., 2009).

5.2 Radar Absorbing

As mentioned before in the paper, various methods have been created to solve EMI-related problems. Radar absorbing materials are produced and used to benefit from the absorbance feature during shielding. The use of magnetic ferrites as microwave absorbers since the World War II is the result of research by J.L. Snoek inspiring German military scientists. In the 1970s, Japanese researchers used magnetic ferrites to create electromagnetic (EM) wave absorbers. The Plessy Company cultivated EM wave absorbers for the British Navy to meet the needs of camouflage and minimize EMI. Composites are widely researched and used to create radar absorbing materials (RAMs) due to their low weight, chemical resistance, high strength-to-weight ratio, customizable design, affordable installation costs, weather resistance, and many other reasons. Metal powders such as graphene, aluminum, zinc, copper, and nickel are frequently used for their great reflectivity, leading to moderate absorption and poor emissivity (Shirke et al., 2024). In the early 1990s, research primarily concentrated on how doping elements affect the magnetic properties of ferrites. Following years, the studies were carried out over a long frequency band range. Lately, there has been a shift in research focus from utlizing rare earth metals as the doping elements instead of metal ions as dopants in ferrites. As examples of some studies: In 1994, Dishovski et al. substituted Co-Ti in Ba-hexaferrite which enhances its microwave absorption. The changes in the components' ratio affect the optimum absorbent thickness within the 8-22 GHz frequency interval. In 1998, Abbas et al. CoSi-substituted Ba-hexaferrite was developed using a solid-state reaction method. The X-band microwave absorption properties of paint coatings of varying thickness was measured by this method. The dual-layer absorber exhibited broadband properties with a 6 dB level across frequencies from 12 to 18 GHz. Meshram et al. (2004) detailed the design, creation, and analysis of hexagonal ferrites as a microwave absorber in the X-band. Their findings revealed broadband traits with minimal absorption of -9 dB spanning from

8.7 to 10.2 GHz for a 2 mm coating thickness in the dual-layer absorber. In 2012, Chang et al. employed the sol-gel citrate method to substitute Ce in barium hexaferrite. They then evaluated the complex permeability & permittivity and microwave absorption characteristics within the 8-13 GHz frequency range. Their observations indicated improved reflection loss at a thickness of 3.5 mm (Kumar and Singh, 2018).

CHAPTER SIX
EXPERIMENTAL STUDIES

6.1 Material Preparations

6.1.1 Substrate Properties

The substrate used in the study is a 0.2 mm thick copper foil tape. Initially 30 x 70 mm samples were cut from the material and then 30 x 90 mm samples were cut for convenience since more samples were needed for characterization measurements and prepared as shown in Figure 6.1. The samples were placed in the experimental setup so that an area of 30 x 40 mm (0.12 dm^2) was coated with alloy.

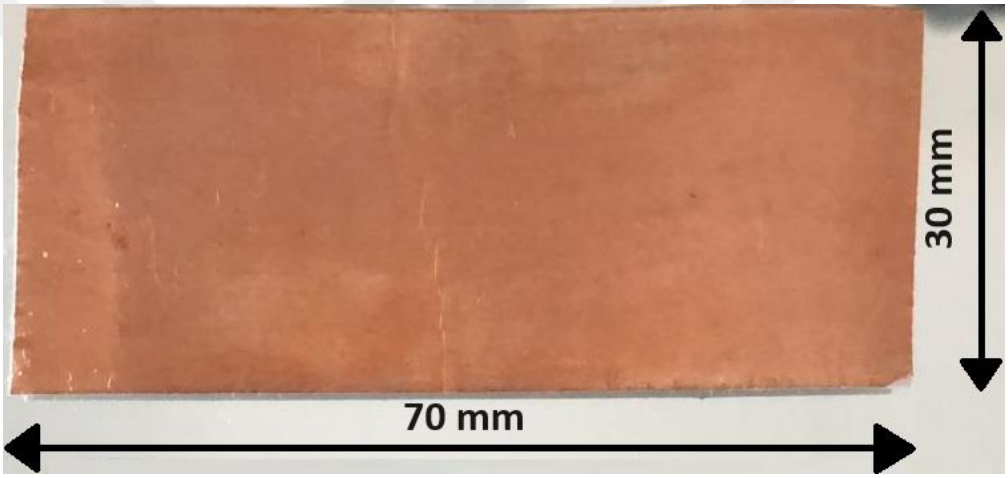

Figure 6.1 Substrate for plating applications

6.1.2 Selection of Chemicals

Since Zn-Ni, Zn-Co, Ni-Co and Zn-Ni-Co will be coated on the substrate, the salts of these metals were used as electrolyte (plating bath) in the proportions specified in Table 6.1. Boric acid (H_3BO_3) and sodium sulfate (Na_2SO_4) were used to balance the pH value. Acetone was preferred to remove the adhesive part of the copper foil tape. Dilute HCl (10%) and distilled water were used in the activation and rinsing processes respectively.

Table 6.1 Plating bath content for each alloy coating

Electrolyte components	**Alloy coating types**			
	Zn-Ni	**Zn-Co**	**Ni-Co**	**Zn-Ni-Co**
$ZnSO_4.7H_2O$	0.25 M	0.25 M	-	0.25 M
$NiSO_4.6H_2O$	0.25 M	-	0.25 M	0.25 M
$CoSO_4.7H_2O$	-	0.25 M	0.25 M	0.25 M
H_3BO_3	0.20 M	0.20 M	0.20 M	0.20 M
Na_2SO_4	0.20 M	0.20 M	0.20 M	0.20 M

6.2 Pretreatment

Before plating, the power supply is checked with the help of a multimeter, and the electrolyte, dilute HCl, distilled water and acetone are placed in different containers. The adhesive part of the copper foil tape is left in acetone for about 5 minutes, and when it is ready, it is removed with the help of a hard object. Then it is rinsed by immersion in distilled water. Afterwards, it is excited in 10% dilute HCl solution and rinsed with enough water. The stated coatings were electroplated in an acidic sulfate bath. Finally, pH measurement is made and the coating process begins. An example setup is shown in Figure 6.2.

Figure 6.2 Sample electroplating mechanism (Personal archive, 2023)

6.3 Plating Process

In this study, as mentioned before, the electroplating method was used, which is easy to prepare, affordable, can be done without the need for high temperature and pressure, and offers high repeability. Two different periods of time were studied: 10 minutes and 20 minutes, in order to obtain data from the products at different coating thicknesses. While a thickness of approximately 11.5-12.5 µm was achieved in 10 minute coatings, a thickness of 22.0-24.0 µm was obtained in 20 minute coatings. Applied current was 0.5 A. Another parameter studied was the current density. After obtaining sufficient data to select a superior coating for further applications, experiments were conducted where the applied current was varied between 0.25 and 2 A. Although the pH value of the solutions was regulated to 3 with the help of dilute sulfuric acid in most experiments, different pH values were also used in recent experiments to increase the data scale. Stainless steel was used as the anode and copper foil tapes were used as the cathode. A power supply with an output voltage of 30 volts, an output current of 6 amps and a fine adjustment mechanism was used. A mechanical

stirrer with adjustable speed was used for the movement of the solution, and the rotation speed of the stirrer used in the experiments was selected as 250 rpm. When the coating process is completed, the coated sample and the material used in the anode are immersed in distilled water and rinsed, the other solution is placed in the plating bath and the processes are continued in the same order until all of them are finished. The flow chart of the process is as in Figure 6.3.

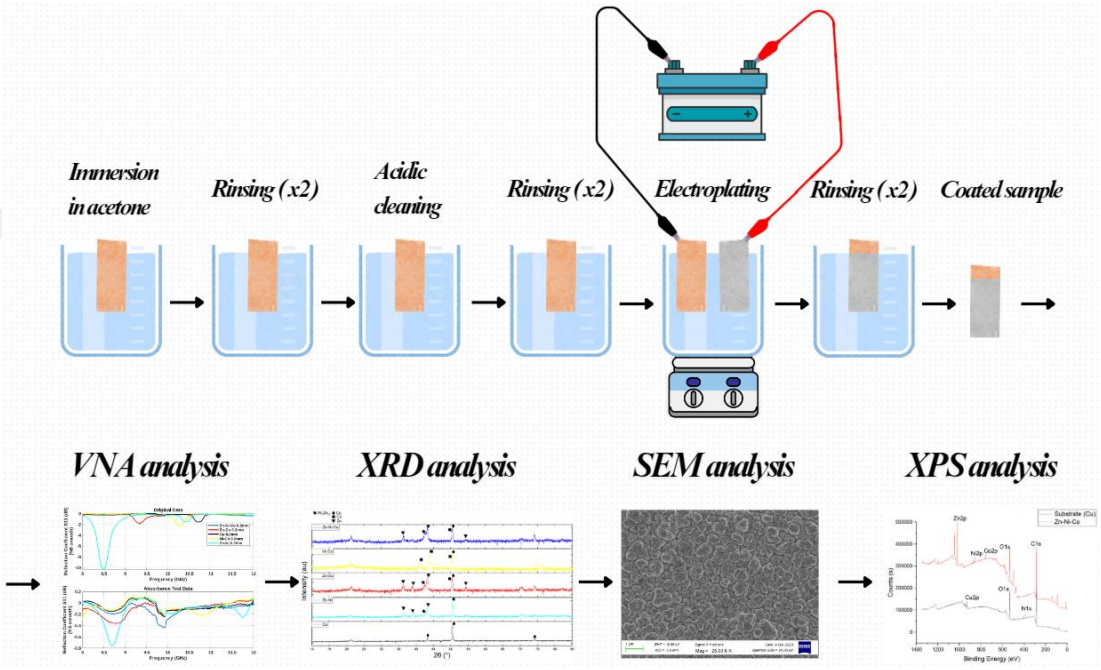

Figure 6.3 Flowchart of electroplating and characterization processes

6.4 Test and Characterization Studies

Cu Kα radiation (60 kV, 60 mA) of the Thermo Scientific brand, ARL X'TRA model X-ray diffraction (XRD) device was used to investigate the phase structures of the plating layers (Fig. 6.4). Data were collected in a 2θ scanning interval from 10 to 85 °, where the step size was 0.020 ° and the divergence angle was 2 °.

Figure 6.4 XRD machine

Scanning electron microscope (SEM) (ZEISS EVO HD15 Plus) (Fig. 6.5) with 20.0 kV acceleration voltage was used for surface morphology and microstructure investigation of the platings. Chemical compositions were determined semi-quantitatively through spot analysis of the coatings using energy dispersive spectrometer (EDS), an apparatus of SEM.

Figure 6.5 SEM machine

For extra information regarding the microanalysis of the coating surface, Thermo Scientific brand, K-Alpha model X-ray photoelectron spectroscopy (XPS) was used (Fig. 6.6).

Figure 6.6 XPS machine

EMI-SE data of coatings on X-band were investigated using a two-port PNA-L - N5230C model vector network analyzer (VNA). The prepared sample (device under test, DUT) was rigidly placed into coaxial waveguide (WR 90, 7-mm) after calibration. S11 (reflection) and S21 (insertion) parameters associated to the electromagnetic features of platings manufactured at varying thickness and the substrate (copper foil tape) were measured in the VNA; then, EMI-SE data in the 8-12 GHz interval were investigated. Figure 6.7 is a demonstration of a basic analysis on VNA. The data was collected graphically through the application afterwards. Obtained data were divided into four different groups called One-Sided Plating, Two-Sided Plating, Two-Sided Thick Plating and Zn-Ni-Co Plating with various current densities, respectively.

Figure 6.7 Basic scattering parameters examination setup: two-port VNA (left), other specimens (right), and DUT (bottom) (Personal archive, 2024)

ElektroPhysik brand eXacto series device (Fig. 6.8) was used for coating thickness measurements.

Figure 6.8 Coating thickness gauge

CHAPTER SEVEN
RESULTS AND DISCUSSIONS

7.1 Group 1 – One-Sided Plating

Four different coatings, namely Zn-Ni, Zn-Co, Ni-Co and Zn-Ni-Co, were coated on a single surface of the substrate for a coating time of 10 minutes. The thicknesses of the coatings on metals are given in Table 7.1.

Table 7.1 Coating thickness (μm) of all coatings

	Zn-Ni	**Zn-Co**	**Ni-Co**	**Zn-Ni-Co**
Group 1 & 2	12.6 ± 1.68	11.9 ± 2.16	12.2 ± 1.89	11.6 ± 2.29
Group 3	22.0 ± 3.89	22.6 ± 2.59	23.5 ± 3.80	24.0 ± 2.86

7.1.1 Characterization of Zn-Ni, Zn-Co, Ni-Co and Zn-Ni-Co coatings

7.1.1.1 SEM examination

The surface morphologies of the electrodeposited coatings were analyzed by examining SEM images shown in Figure 7.1. EDS results (Figure 7.2) indicate that the percentages of Zn, Ni and Co in the coatings vary. Zn-Co coating, is the one which Zn content peaked, while the Ni-Co coating had a significantly higher Co content. The surface morphologies of the Zn-Co and Zn-Ni coatings are identical, primarily due to the high Zn content in both. However, the appearance of the surface of the Zn-Co coating is different from the other coatings in SEM images (Figure 7.1.c, 7.1.d). The surface morphology of the Ni-Co deposition (Fig. 7.1.e, 7.1.f) is characterized by smooth, spherical, fine-grained nodules, typical of Co alloys. In Figure 7.1.g, the Zn-Ni-Co coating demonstrates a more uniform and dense structure.

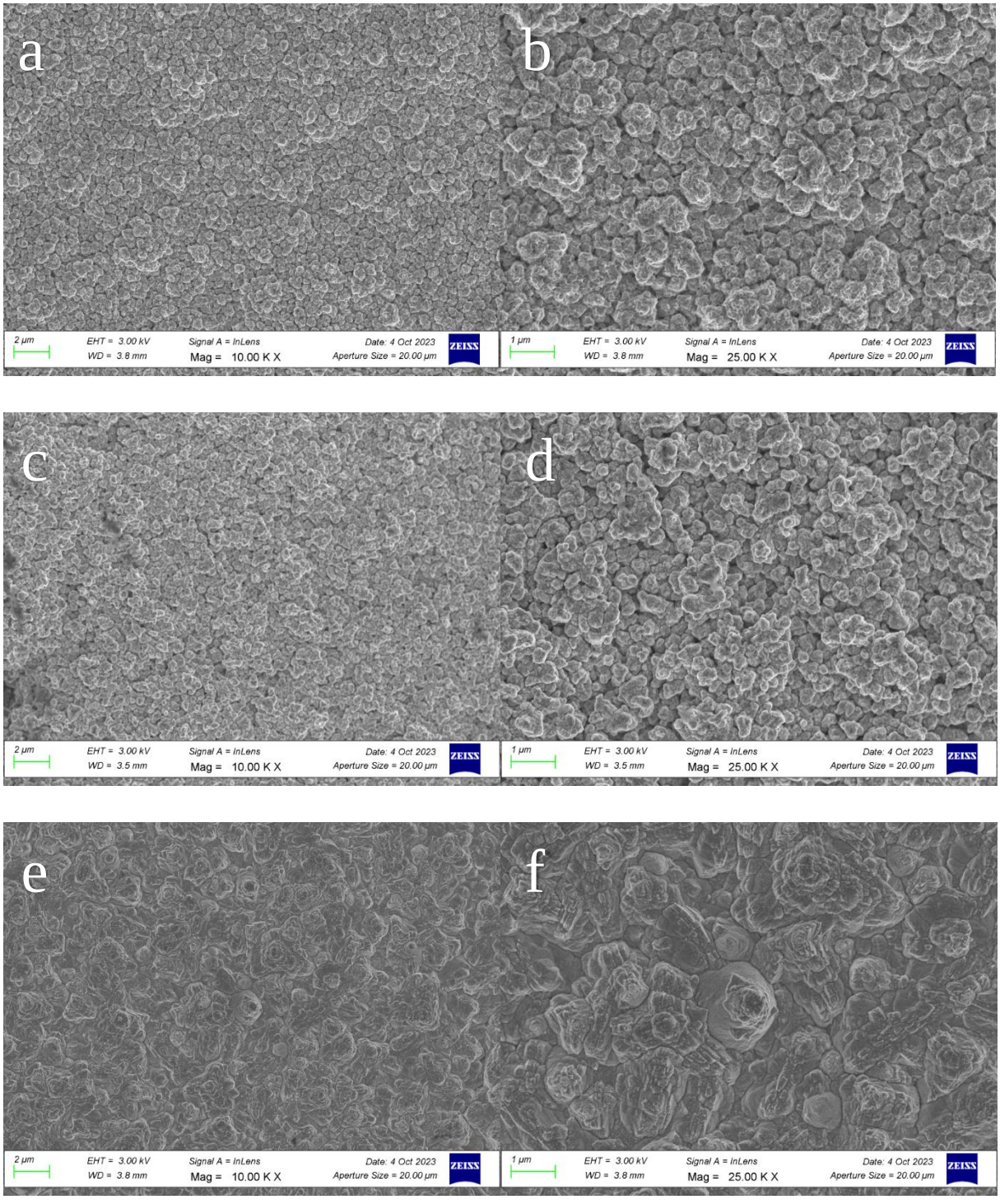
a
2 µm
EHT = 3.00 kV
WD = 3.8 mm
Signal A = InLens
Mag = 10.00 K X
Date: 4 Oct 2023
Aperture Size = 20.00 µm
ZEISS
b
1 µm
EHT = 3.00 kV
WD = 3.8 mm
Signal A = InLens
Mag = 25.00 K X
Date: 4 Oct 2023
Aperture Size = 20.00 µm
ZEISS
c
2 µm
EHT = 3.00 kV
WD = 3.5 mm
Signal A = InLens
Mag = 10.00 K X
Date: 4 Oct 2023
Aperture Size = 20.00 µm
ZEISS
d
1 µm
EHT = 3.00 kV
WD = 3.5 mm
Signal A = InLens
Mag = 25.00 K X
Date: 4 Oct 2023
Aperture Size = 20.00 µm
ZEISS
e
2 µm
EHT = 3.00 kV
WD = 3.8 mm
Signal A = InLens
Mag = 10.00 K X
Date: 4 Oct 2023
Aperture Size = 20.00 µm
ZEISS
f
1 µm
EHT = 3.00 kV
WD = 3.8 mm
Signal A = InLens
Mag = 25.00 K X
Date: 4 Oct 2023
Aperture Size = 20.00 µm
ZEISS

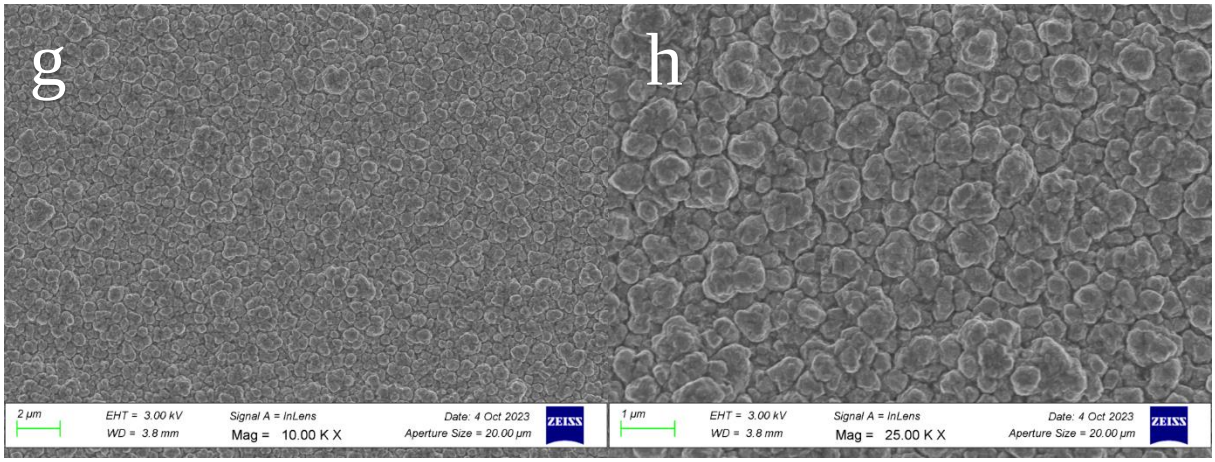

Figure 7.1 SEM photographs of (a, b) Zn-Ni plating, (c, d) Zn-Co plating, (e, f) Ni-Co plating and (g, h) Zn-Ni-Co plating

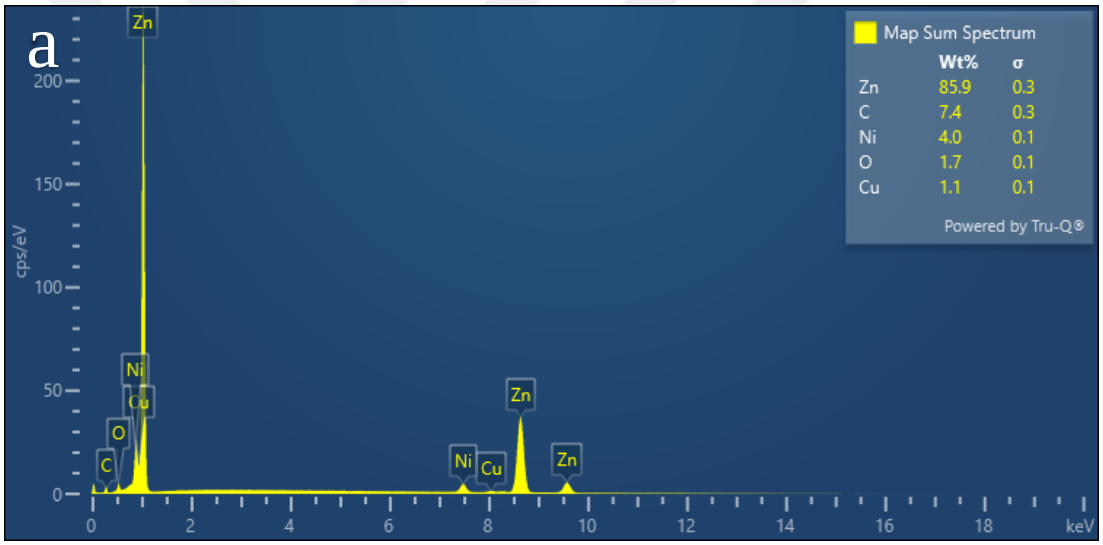

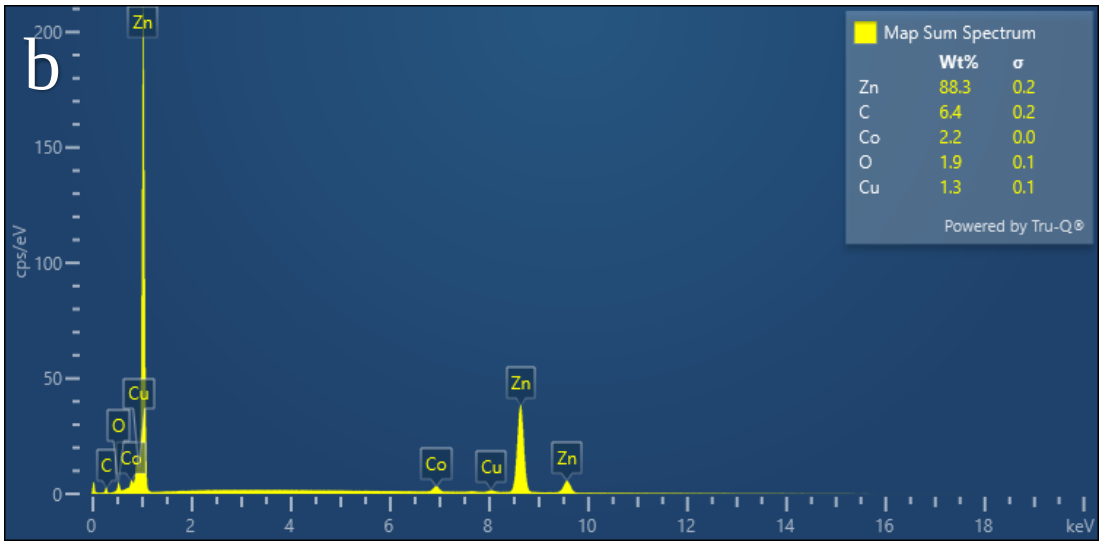

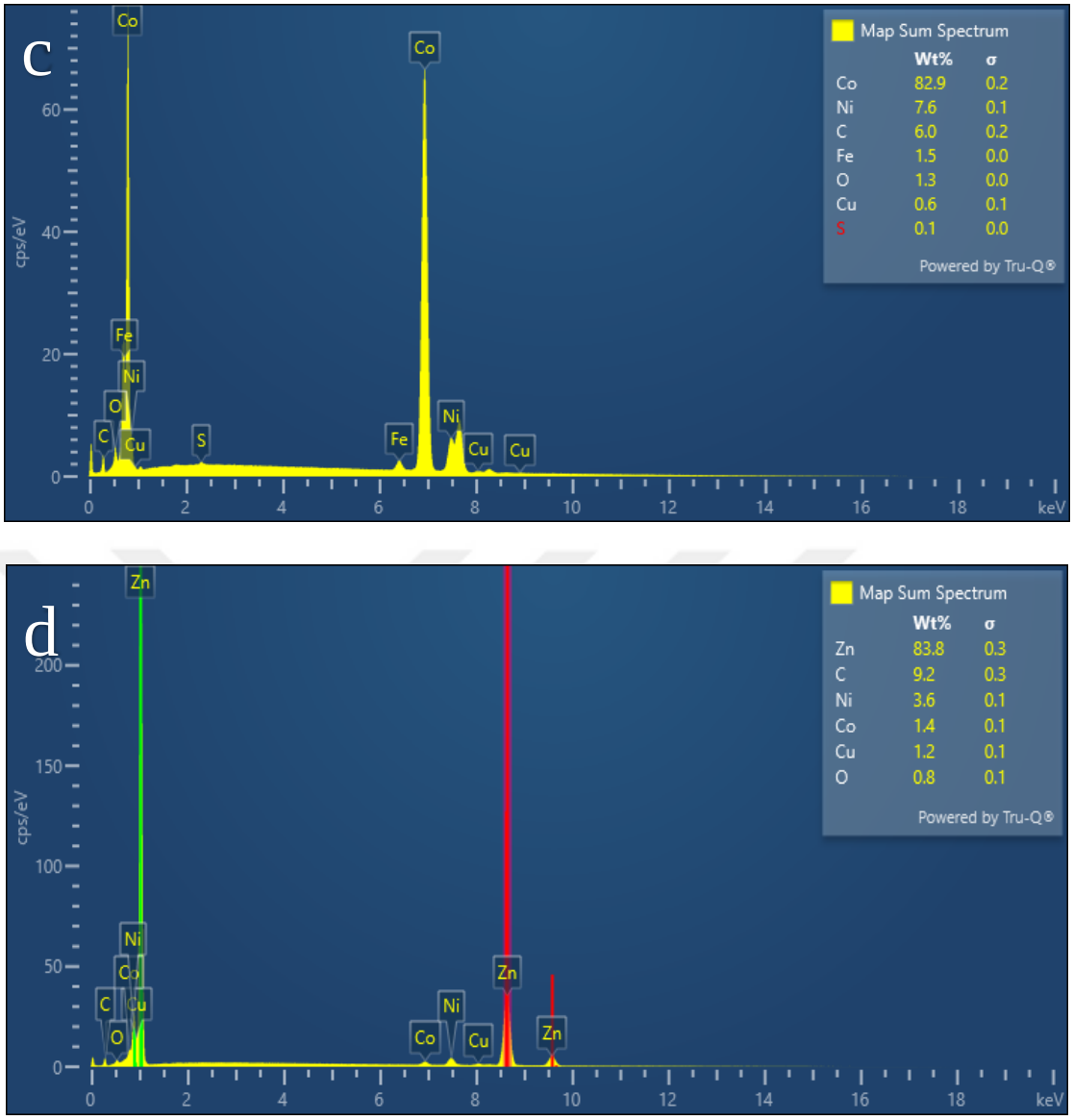

Figure 7.2 The EDS results of (a) Zn-Ni plating, (b) Zn-Co plating, (c) Ni-Co plating and (d) Zn-Ni-Co plating

7.1.1.2 XRD studies

XRD patterns of alloy coatings on copper foil are illustrated in Figure 7.3. The superior peak at 2θ=50.4° in each specimen corresponds to the substrate. The Zn-Ni alloy coating can exhibit three diverse phases, η (a solid solution of Ni in Zn), α (a solid solution of Zn in Ni), and γ (intermetallic compound Ni_5Zn_{21}), which are affected by the amount of Ni and accumulation conditions. The peaks observed at 2θ=36.40°, 2θ=39.06°, 2θ=42.56° and 2θ=43.30° correspond to pure Zn, γ and η-Zn phases, respectively. Although γ (2θ=57.06°) is missing due to the low Ni amount (4 wt. %),

some phases are present in the coating. According to several statistics in the literature, only supersaturated η-phase is occured in Zn-Ni coatings with Ni contents up to 7 wt%. Coatings accumulated from a temperature of 60 °C chloride bath contain supersaturated η-phase. In Zn-Co coatings, where the composition includes the η-phase and the solubility of Co in zinc is approximately 3%, the amount of Co is low. Given that the Co content in the Zn-Co alloy coating is 2.2 wt. %, the three peaks at 2θ=36.28°, 2θ=38.92°, and 2θ=43.28 ° confirm this phenomenon. The phase structures of Ni-Co alloys can shift between hexagonally close-packed (hcp) and face-centered cubic (fcc), determined by the changing weight ratios of Ni and Co in the coating. In this case, not only is Co significantly greater than Ni, with peaks at 2θ=41.34° and 2θ=44.21°, but it also makes up more than 80% of the solution, resulting in a predominantly hcp structure. The XRD data of the Zn-Ni-Co coating is fairly different from the classical structure of its constituents as it covers all binary combinations simultaneously. Nearly all phases of Zn-Ni, Zn-Co and Ni-Co platings in ternary coatings are denser than in binaries. The contrast between these outcomes and those indicated in the literature is likely to be due to the varying conditions under which the coatings were deposited. Nearly all phases in the Zn-Ni-Co alloy coating appear more prominently than in the binary versions. The contrasts between the outcomes noted in the literature and those obtained from experiments are thought to be due to the different

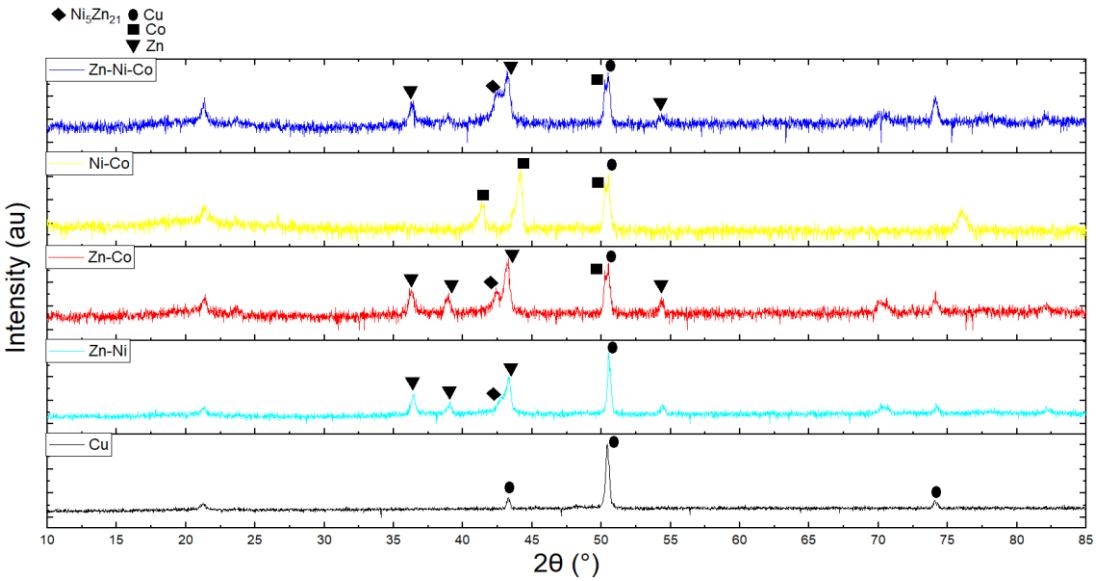

ambient conditions under which the coatings were produced.

Figure 7.3 XRD patterns of the copper substrate and its plated states using Zn–Ni, Zn–Co, Ni–Co, and Zn–Ni–Co metal alloys

7.1.1.3 XPS studies

Elemental percentages in the XPS survey spectra are demonstrated in Table 7.2. It is clearly seen that all the specimens primarily contain Cu, Zn, Ni, Co, O, and C elements (Figures 7.4-7.7).

The photoelectron peaks appear distinctly at the following binding energies: Cu2p at 935 eV, Zn2p at 1045 and 1023 eV, Ni2p at 855 eV, Co2p at 780 eV, O1s at 531 eV, and C1s at 285 eV. Since some adventitious hydrocarbons exist in the XPS instrument, C1s peak, serving as an internal standard was easily detected. The peak positions align well with the values noted in the literature (Chen et al., 2015; Jiang et al., 2021).

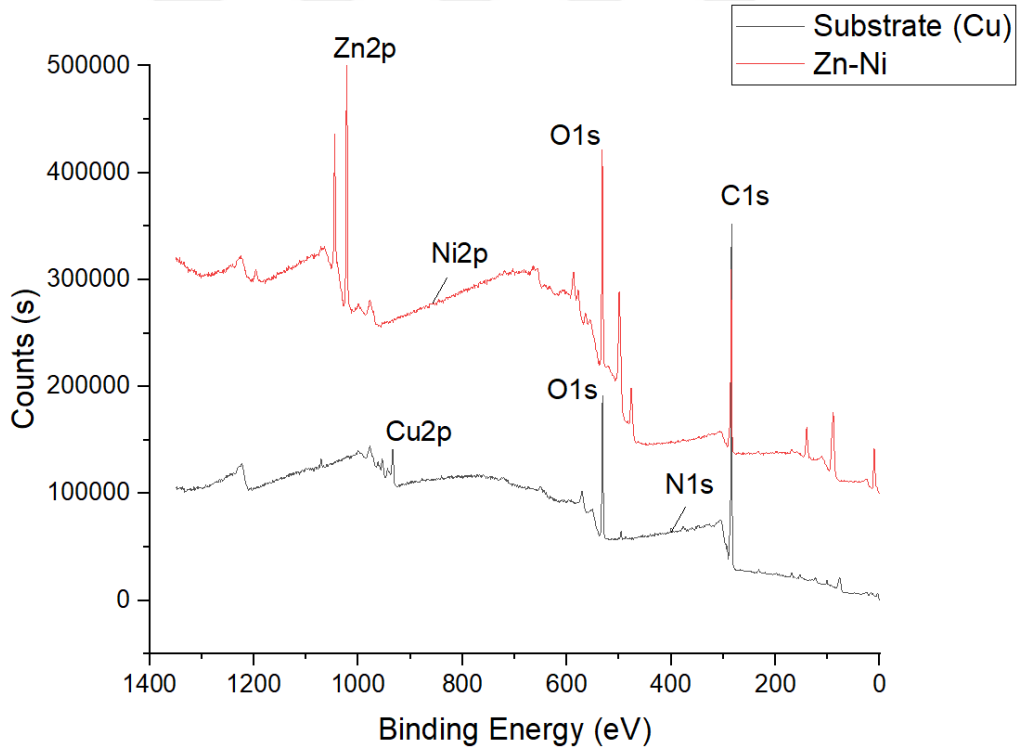

Figure 7.4 XPS survey spectra of Zn-Ni alloy coating – substrate

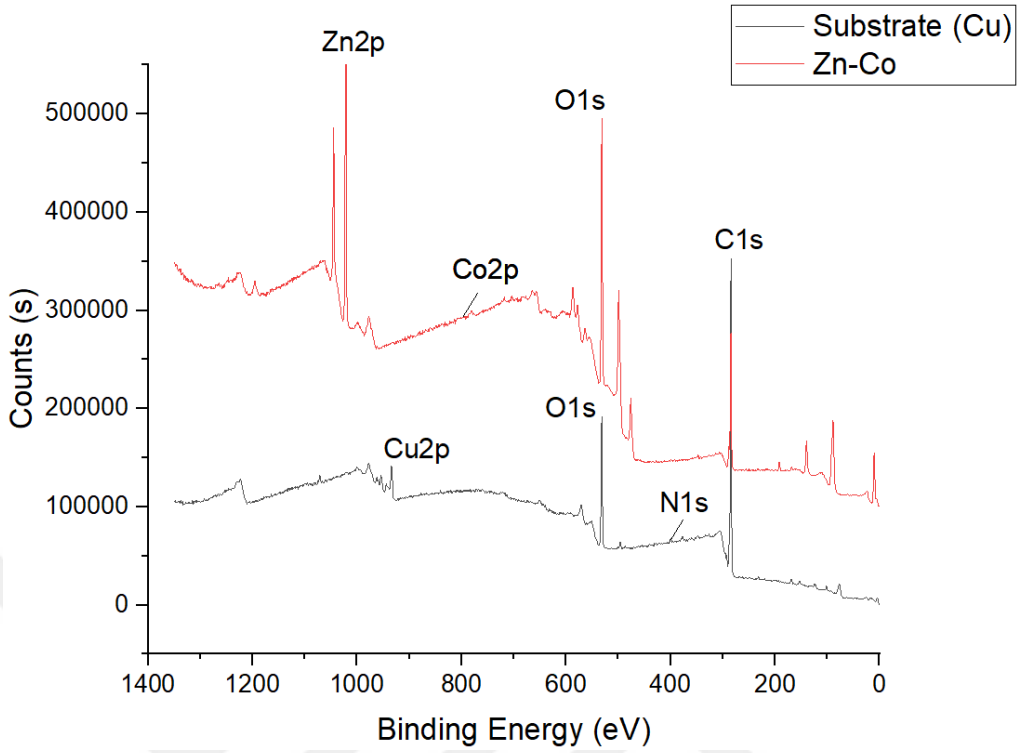

Figure 7.5 XPS survey spectra of Zn-Co alloy coating – substrate

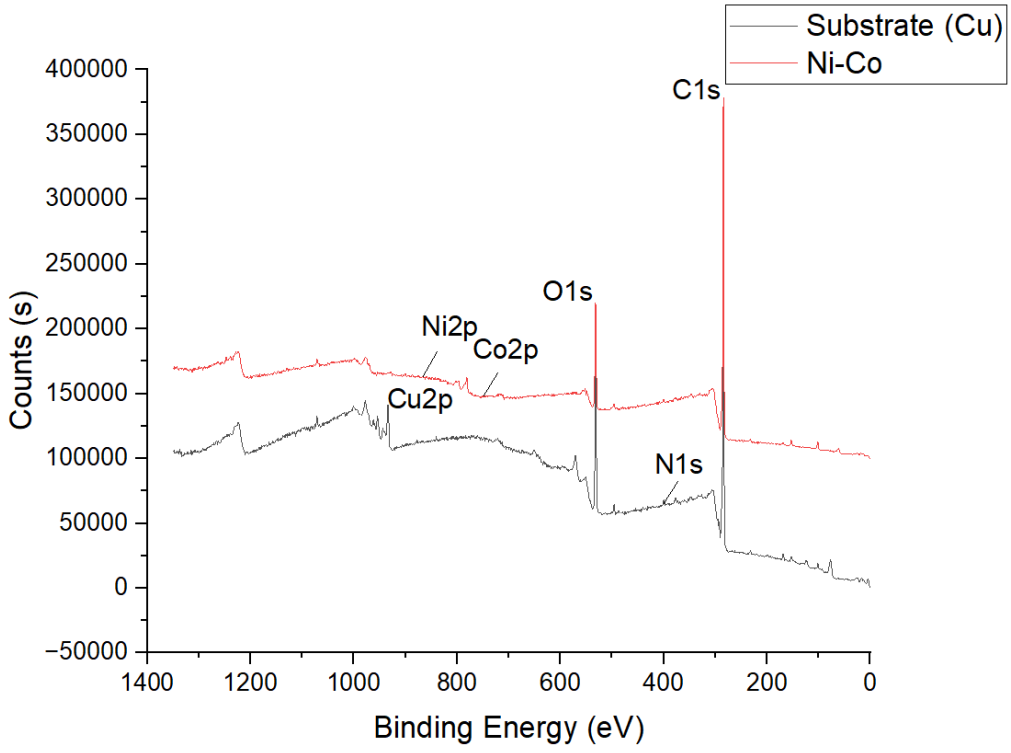

Figure 7.6 XPS survey spectra of Ni-Co alloy coating – substrate

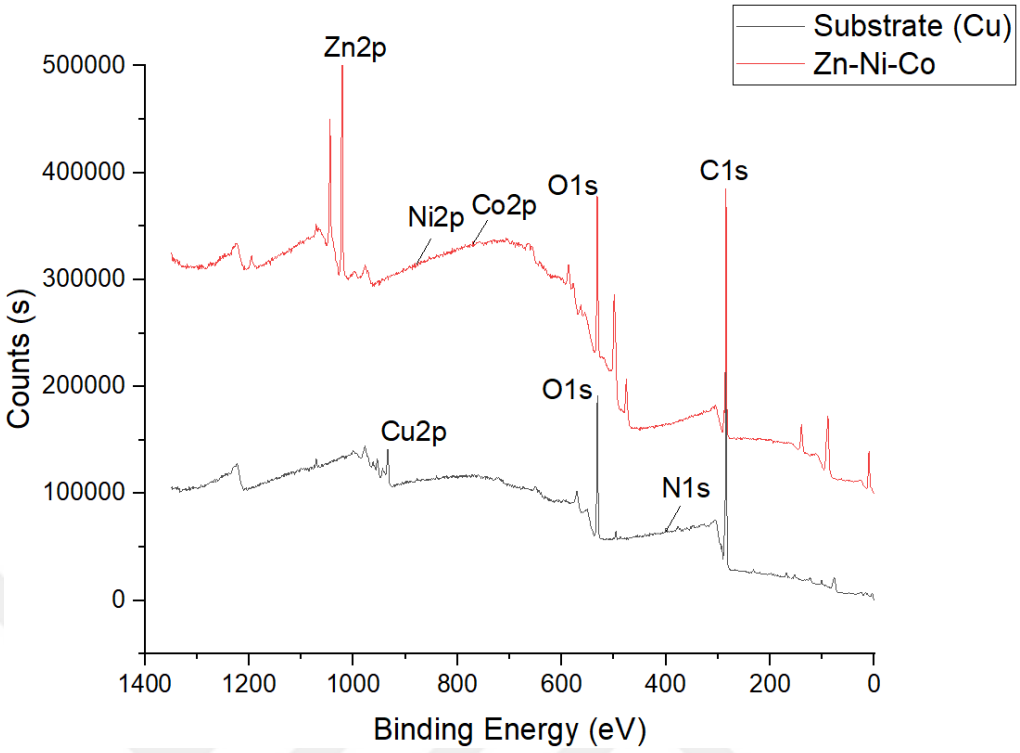

Figure 7.7 XPS survey spectra of Zn-Ni-Co alloy coating – substrate

Table 7.2 Atomic concentration of elements (%wt) from XPS survey data

	Zn-Ni	**Zn-Co**	**Ni-Co**	**Zn-Ni-Co**
Zn	38.10	39.82	-	33.31
Ni	0.79	-	1.07	1.06
Co	-	1.54	5.43	0.72
C	35.33	29.27	72.83	46.59
O	23.98	28.18	14.67	18.32
Others	1.80	1.19	6.00	0

7.1.2 VNA studies

7.1.2.1 EMI-SE examination

S parameters (S11, S21) of all specimens are shown in Fig. 7.8. The lines are sharpened by applying a softening process to them. Despite slight undesirable shifts in the graph, the coatings improved the performance of the substrate overall. This is because the individual gain (dB) from the products has shifted towards -∞. Although this might seem counterintuitive, since shielding opposes electromagnetic interference (a negative phenomenon), a decrease in the gain is a reasonable outcome. In fact, as the lines move downwards on the chart, the gain effectively increases.

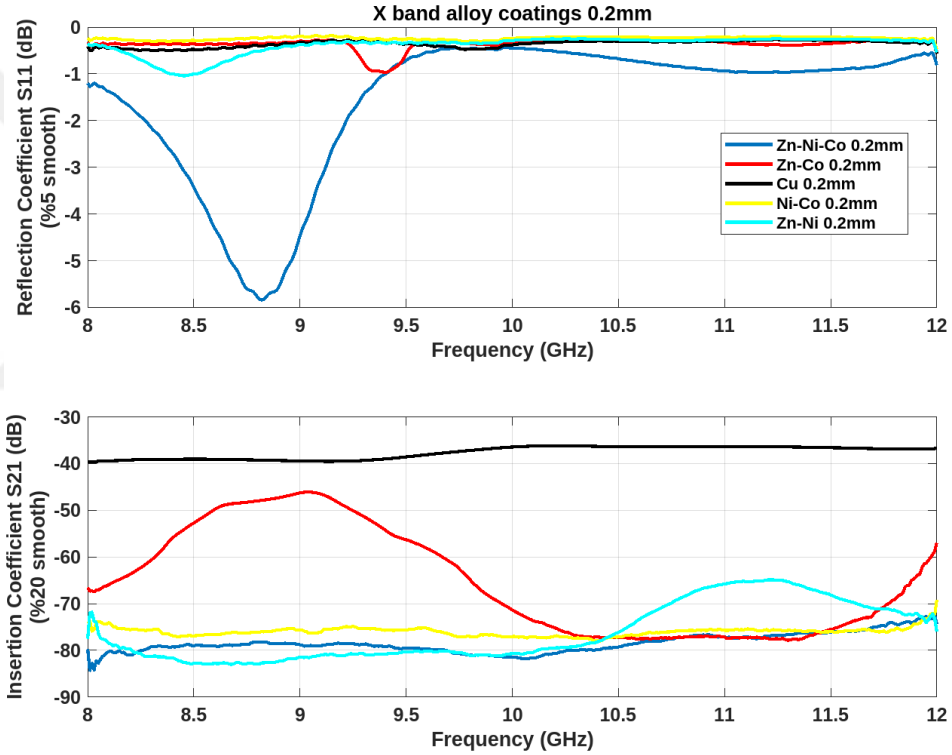

Figure 7.8 Reflection (S11) – insertion (S21) data of platings and substrate (Group-1)

Because of the placement of the sample between two ports of the VNA, EMI-SE is related with the sample's insertion coefficient, which was mentioned before in this paper. According to ASTM ES7-83 Standard, SE (dB) can be calculated with the aid of scattering parameters (S parameters) S21S and S21E, portraying the evaluations with and without the sample which are called S (sample) and E (empty), respectively.

$$SE(dB) = S21E(dB) - S21S(dB) \tag{7.1}$$

Equation (7.1) provides the basic calculation for SE (dB). In theory, the gain value that determines whether a material is intended for shielding of general materials is evaluated through certain limits: typically, shielding is 50% efficient at -3 dB, 70-90% efficient at -7-10 dB, 90-99% efficient at -10-20 dB, 99.0-99.9% efficient at -20-30 dB and approximately 99.9% efficient at -30 dB. The overall electromagnetic interference shielding effectiveness - shielding percentage relationship between values of 70-99.9% for general materials is shown in Table 7.3 (Mishra et al., 2018). The goal is to increase the gain as much as numerically possible without '-' to maximize shielding efficiency around 99.9999...%, aiming for an ideal value of 100% efficiency. The S21 data for all samples, including the holder (empty state), is shown in Figure 7.9. Therefore, the SE (dB) values of the coatings are calculated by substituting the data in Figure 7.9 into Equation (7.1). This method is chosen because the S21 value of the holder (empty) is very close to 0 dB and the SE (dB) graphs usually show the values as positive numbers. Upon examination of the specimens, it was noticed that despite disparities among them, they all exhibited superior shielding effect than copper.

Table 7.3 EMI-SE and its associated shielding percentage values

EMI-SE (dB)	Electromagnetic Shielding (%)	Performance of Materials
EMI-SE > 30	Electromagnetic shielding > 99.9	Excellent
30 ≧ EMI-SE > 20	99.9 ≧ Electromagnetic shielding > 99.0	Very Good
20 ≧ EMI-SE > 10	99.0 ≧ Electromagnetic shielding > 90	Good
10 ≧ EMI-SE > 7	90 ≧ Electromagnetic shielding > 70	Fair (70-80 dB), Moderate (80-90 dB)

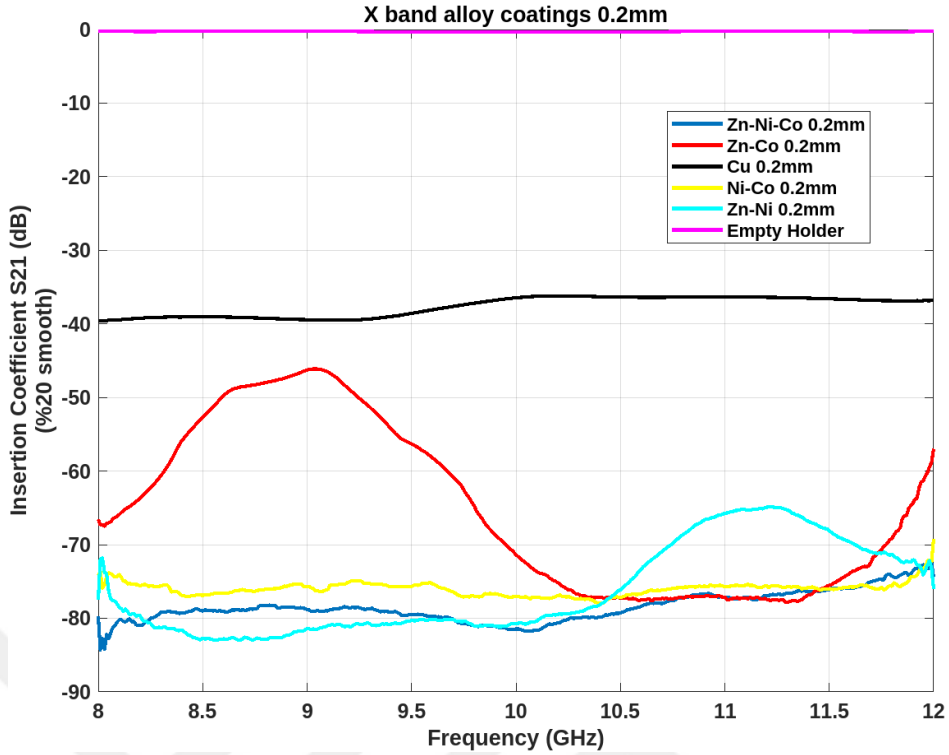

Figure 7.9 Insertion (S21) values of platings, substrate and holder (empty)

Zn-Co has the lowest shielding effect among the other samples, as evidenced by the fact that its graph is quite fluctuating. While all samples generally fall within a good yield range, the Zn-Ni-Co alloy ultimately provides the best yield, as shown in Table 7.4. In addition to the graph, this table describes the efficiency offered by the examples based on specific priorities. The evaluation starts by examining the mean values in the given order. The highest and lowest values are then compared to identify two decent examples with similar data. The standard deviation and the range of data at a given point are taken into account when previous information is not sufficient to decide which is the most efficient specimen.

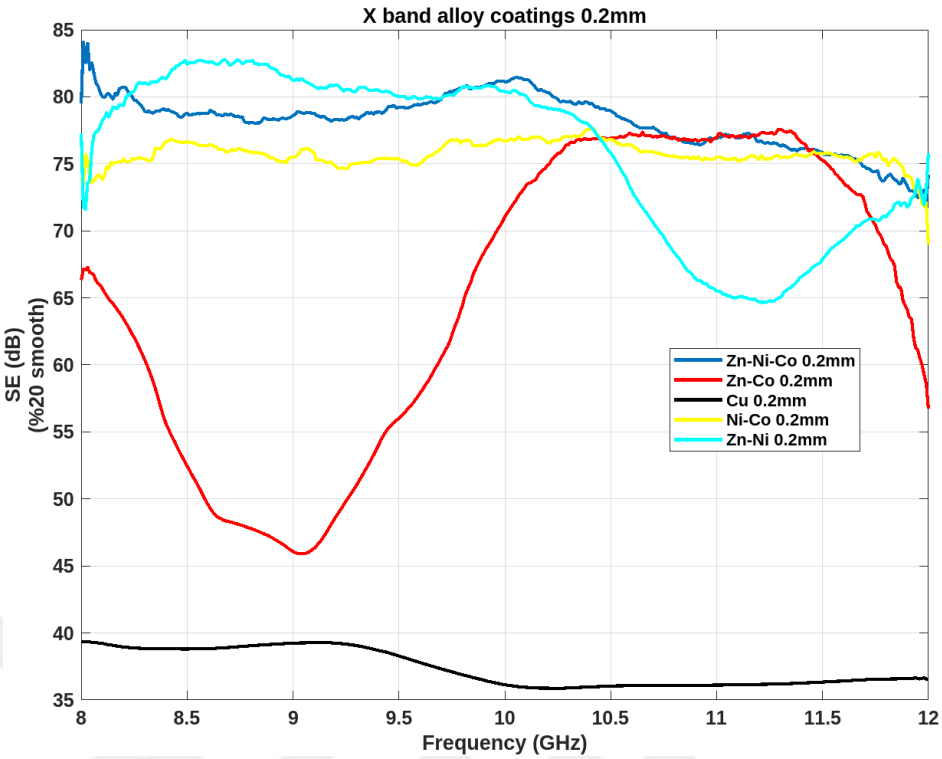

Figure 7.10 SE (dB) data of platings (Group-1)

In Figure 7.10, which cumulatively shows the results obtained using Eq. (1), all four materials demonstrate notable shielding effects at certain frequencies. Given that minimal fluctuation is desired, the Zn-Ni-Co sample shows the best efficiency. As mentioned earlier, it is important to understand that the data of all specimens is within the desired interval and increases the shielding value of the substrate. Therefore, it makes sense to use the better performing materials. The most efficient ones are noted after each experiment.

7.1.2.2 Absorbance

In order to analyze the absorbance values of the coatings, the system was short-circuited by placing a thin plate (aluminum) between the specimen and the signal meter during the sample preparation phase and the experiments were conducted in this way. Figure 7.11 presents both the initial S11 data (in Figure 7.8) and the data obtained after absorbance testing. There was no significant difference in terms of numerical value before and after the analysis, but noticeable changes were observed in terms of shape. However, instead of scattered and varyingly rising and falling values, a data group that

changes within a narrower range appears on the graph, which is a sign that the data, although numerically weak, is obtained in the desired direction.

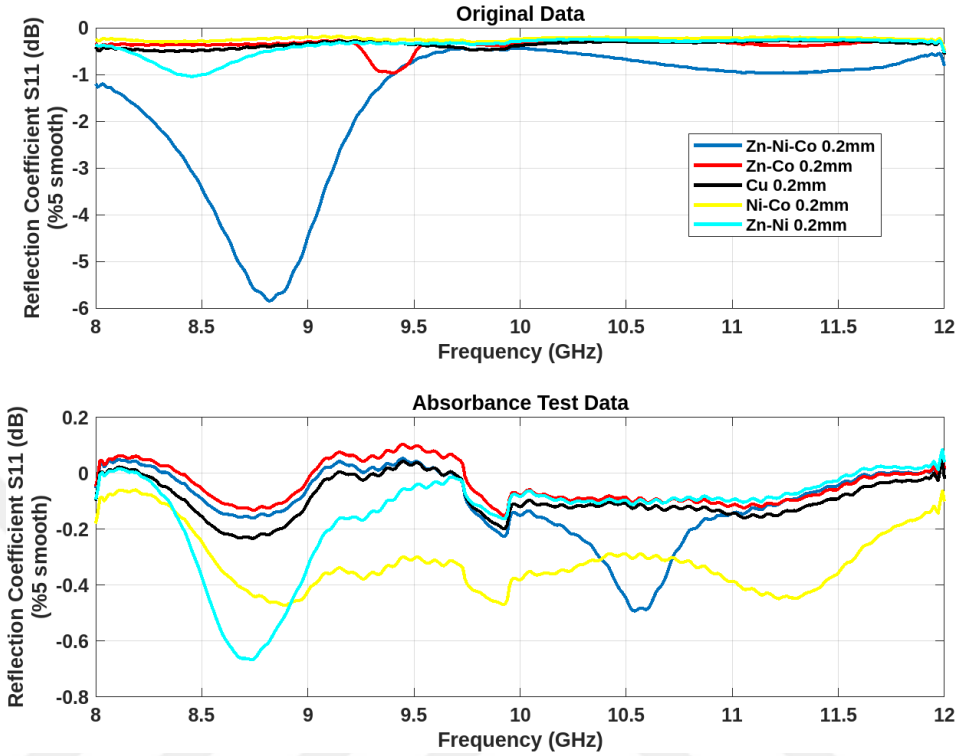

Figure 7.11 Absorbance (S11) values of platings and substrate (a) original, (b) after absorbance test (Group-1)

When Figure 7.11 (a) is examined, the absence of specific movement is expected because, as known, the absorbance behavior test typically requires a material like aluminum. The minor fluctuation observed on the Zn-Ni-Co data can appear under various conditions and is not significant. After the test in which the second port was short-circuited, it can be seen that the substrate and the other specimens exhibit mostly the same behavior in the frequency range in 7.11 (b). In evaluating shielding, it was detected that the Ni-Co alloy demonstrated the highest absorption effectiveness, as indicated by Table 7.5 and the Figure 7.11 together.

7.2 Group 2 – Two-Sided Plating

Unlike the previous experiments, in this group the coating was applied to both surfaces of the substrate. The coating time was kept at 10 minutes.

7.2.1 Characterization of Zn-Ni, Zn-Co, Ni-Co and Zn-Ni-Co coatings

Since the experiments were performed with the same parameters as group 1, no significant change was observed during characterization. In this group, the back surface of the copper substrate was coated under the same conditions as the experimental parameters of group 1. Therefore, there is no variability in terms of surface structure and morphology. The effect of double-sided coating on electromagnetic shielding was investigated.

7.2.2 VNA studies

7.2.2.1 EMI-SE examination

While producing the samples in the second group, both sides of the substrate were coated as a difference. It was noticed that the efficiency of Zn-Ni-Co, which gave the highest performance last time, decreased while that of Zn-Co, which gave the lowest performance, increased. Although there were undesirable fluctuations in all of them, it was determined that Ni-Co exhibited the best shielding efficiency as a result of this experiment, by examining the Figure 7.12 and Table 7.4 together, in the same way as the previous ones. In any case, it is obvious that there has been an overall improvement after the highs and lows.

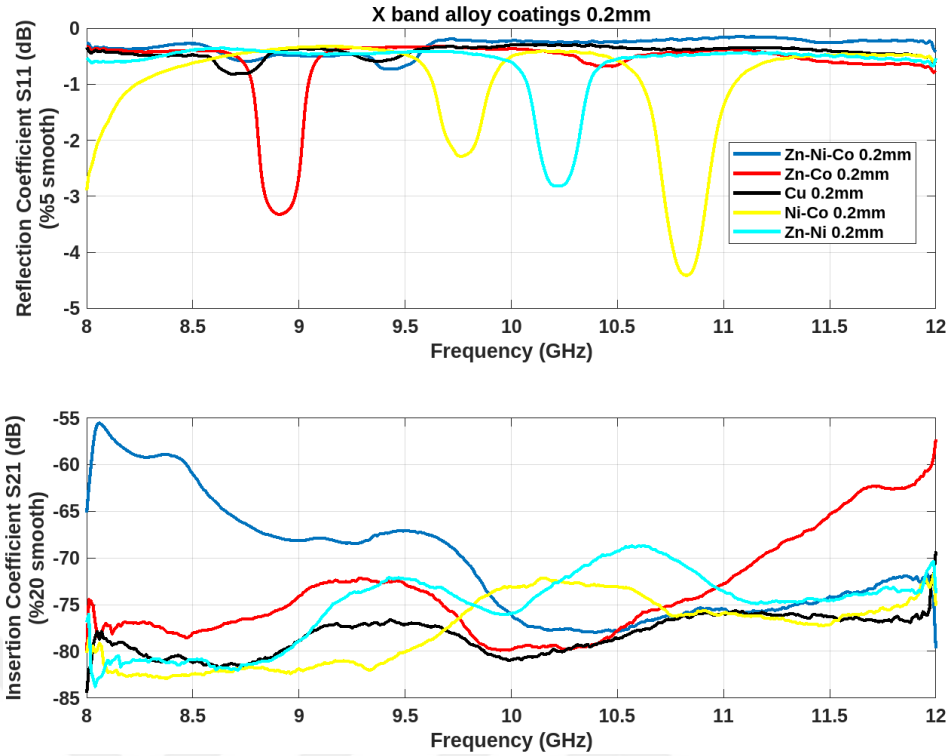

Figure 7.12 Reflection (S11) – insertion (S21) data of platings and substrate (copper foil tape) (Group-2)

Since the value of the holder is 0 dB (Figure 7.9), Eq. (1) was directly used in the SE evaluation of this group. Compared to group 1, although the upper limit of the SE values in group 2 is close, the lower limit is higher in terms of gain, which is evidence of general improvement as mentioned before. In the parts that seem to have relatively low gain in the Figure 7.13, decent efficiency was actually obtained when considered from the scale used for evaluation. As a result, it can be said that Ni-Co has the best efficiency compared to the substrate.

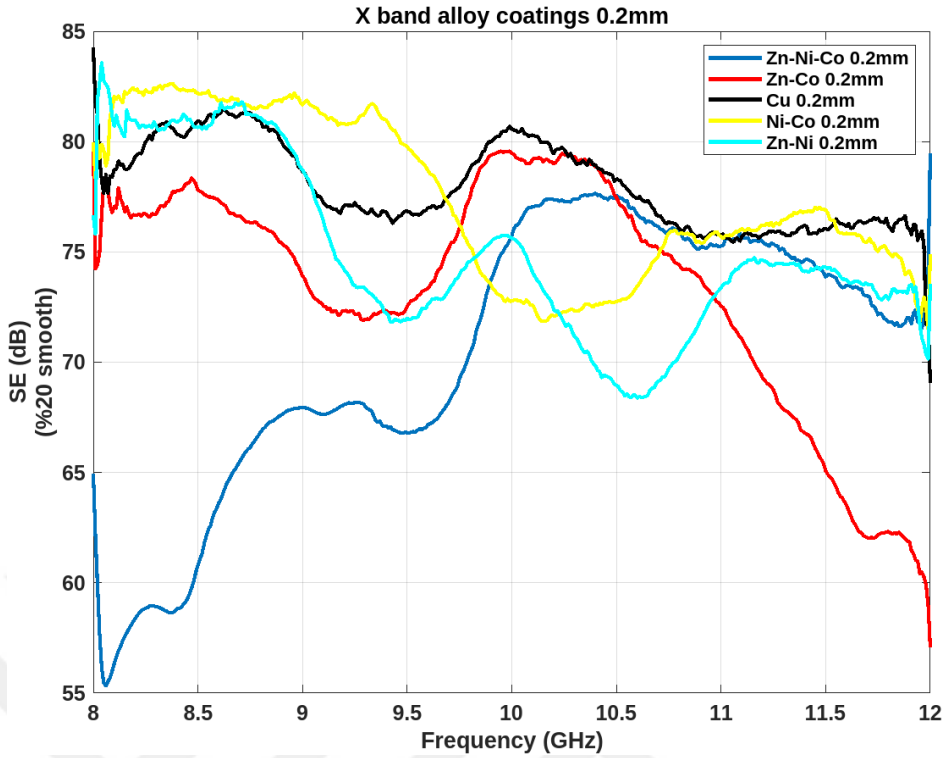

Figure 7.13 SE (dB) data of platings (Group-2)

7.2.2.2 Absorbance

Since it is the same coating as Group 1, prepared on both sides instead of one side, the absorbance result is naturally similar. Therefore, when looking at Figure 7.14, the results in 7.14 (a) are numerically similar to group 1, except for certain increases. Since there will be no excessive difference in 7.14 (b), it is seen that the most efficient material in terms of absorbance is again the Ni-Co alloy coating.

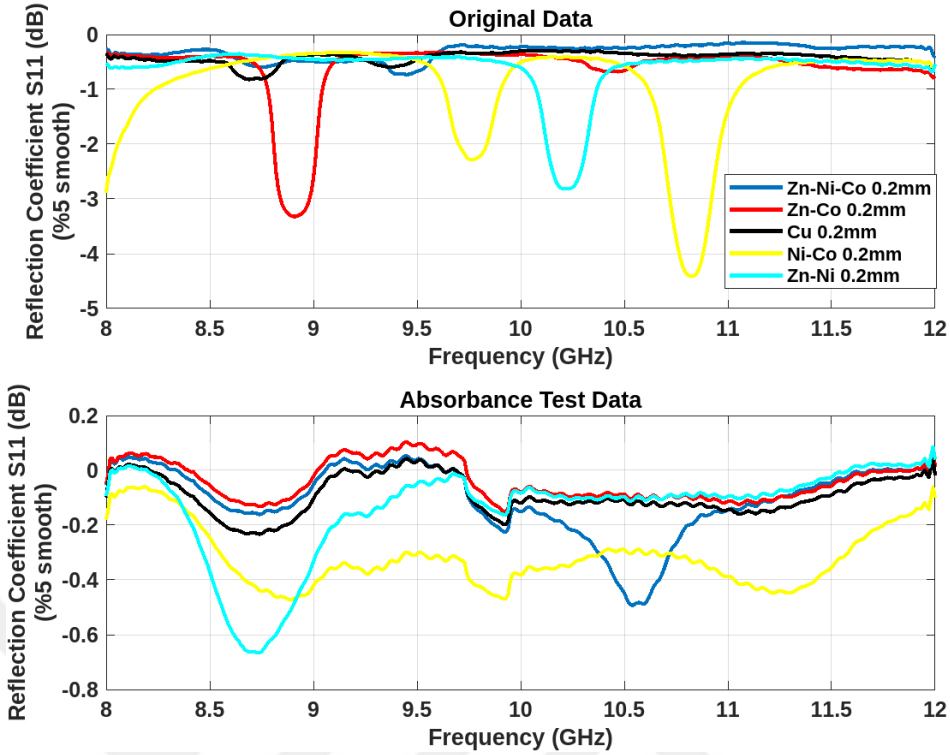

Figure 7.14 Absorbance (S11) values of platings and substrate (a) original, (b) after absorbance test (Group-2)

7.3 Group 3 – Two-Sided Thick Plating

Unlike group 2, the coatings were performed in 20 minutes instead of 10 minutes. The remaining parameters are the same as the previous groups.

7.3.1 Characterization of Zn-Ni, Zn-Co, Ni-Co and Zn-Ni-Co coatings

Since the experiments were performed with the same parameters as group 1 and group 2, no significant change was observed during characterization.

7.3.2 VNA studies

7.3.2.1 EMI-SE examination

When the shielding data is examined, it is understood that the gain values in group 3 are generally better than the previous ones. Although single-sided, double-sided and finally thicker coatings have undesirable results in some regions of the X band frequency range, they are observed to be performance enhancing steps when viewed

from a broad perspective. In this experimental group, the samples have values closer to each other in most of the frequency range than in previous runs. Although it is not exactly clear from Figure 7.15 that which one is the best, a small evaluation based on the Table 7.4 shows that Zn-Ni-Co has better shielding efficiency for group 3, where thick coating is applied.

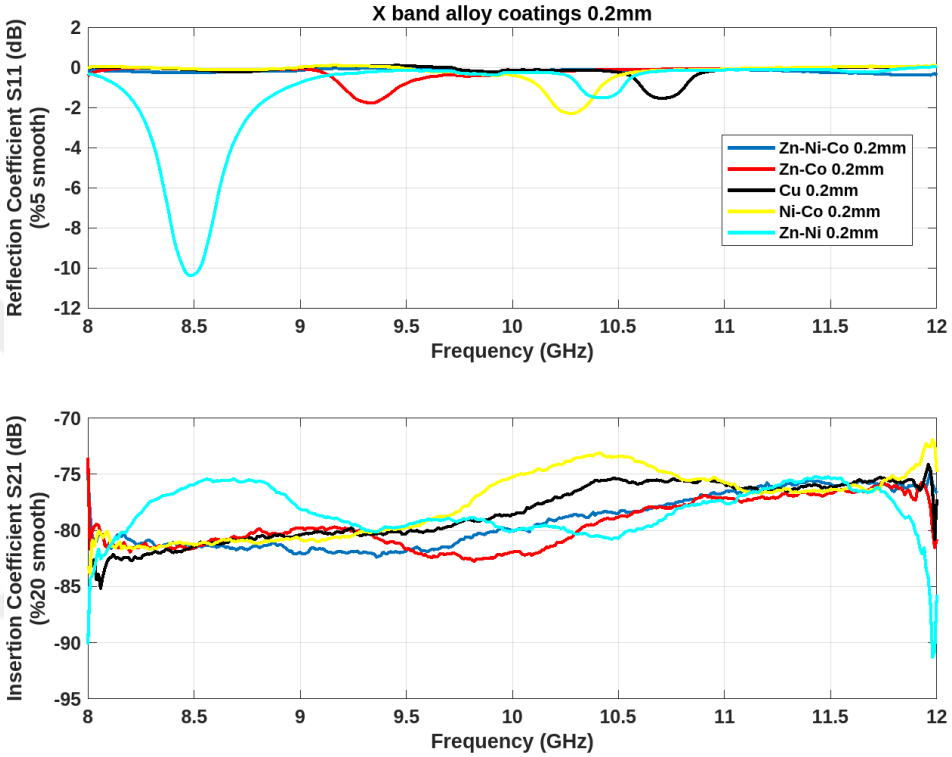

Figure 7.15 Reflection (S11) – insertion (S21) data of platings and substrate (copper foil tape) (Group-3)

While making SE evaluation, Eq. (1) was used directly. Compared to previous experiments, although the values increased considerably in certain regions of the frequency range, especially for Zn-Ni, long-term efficiency could not be achieved in this group. For this reason, it can be said that the Zn-Ni-Co sample has better SE values with the usual evaluation method using the Figure 7.16 and Table 7.4 together.

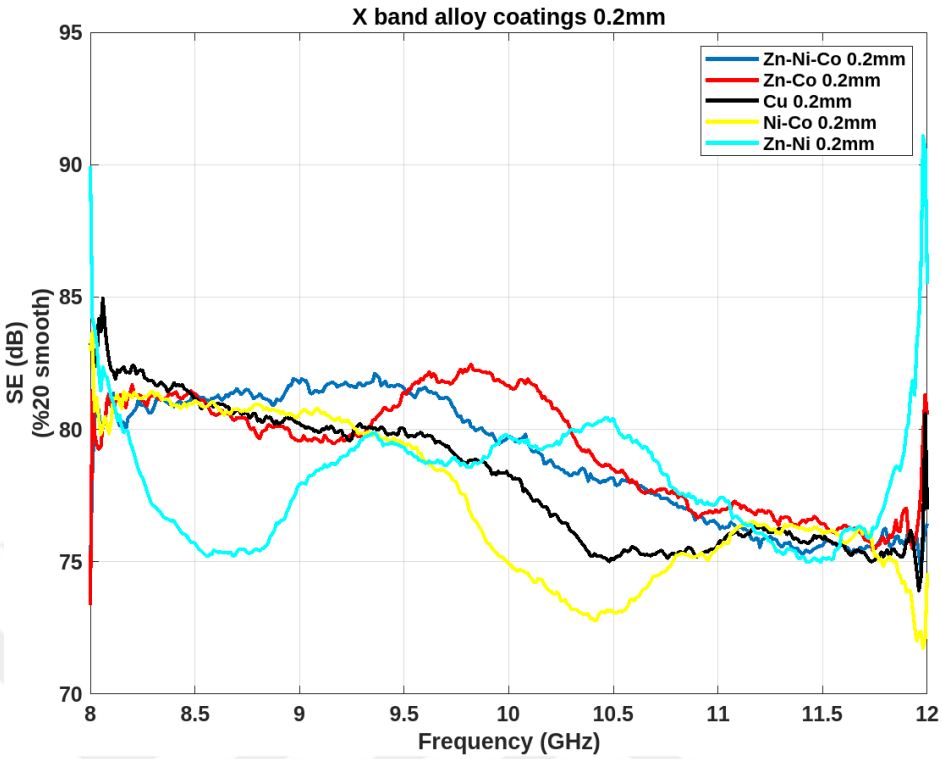

Figure 7.16 SE (dB) data of platings (Group-3)

7.3.2.2 Absorbance

When the coatings in group 3, which were thicker in addition to the double-sided coating as in group 2, were examined, it was observed that the absorbance values were again in a similar range. In the results of group 2, except for Ni-Co, which stands out in particular, the remaining samples are almost the same, while the difference is a little more pronounced in this experimental group. As always, except for fluctuations in certain areas, it was determined from the Figure 7.17 and Table 7.5 that Zn-Ni-Co has better absorbance.

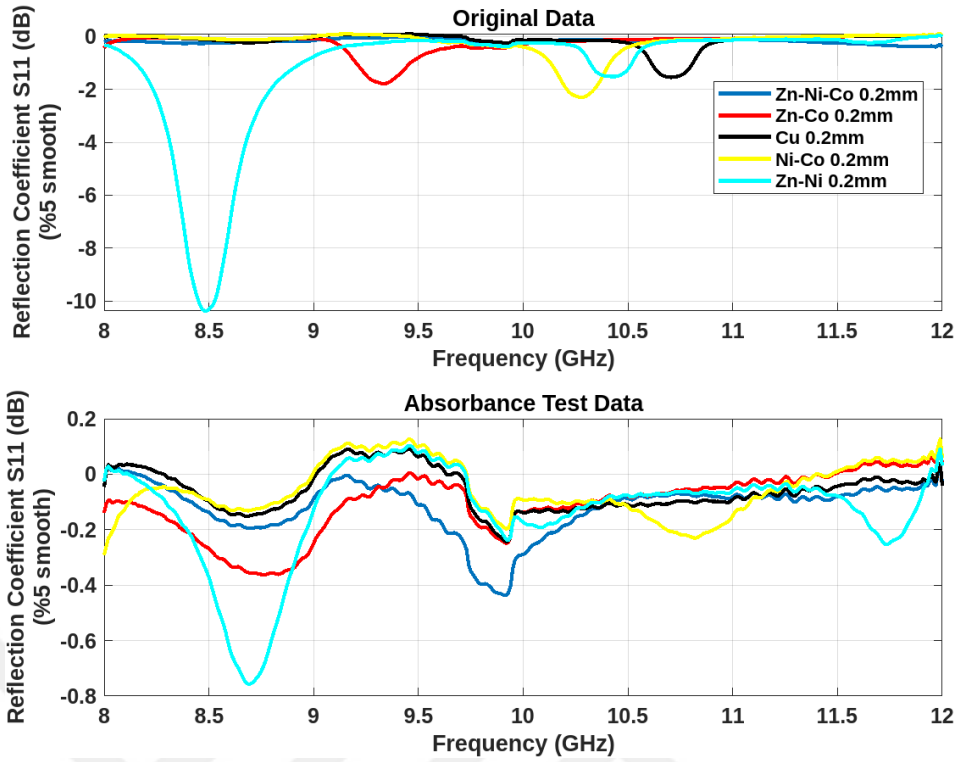

Figure 7.17 Absorbance (S11) values of platings and substrate (a) original, (b) after absorbance test (Group-3)

7.4 Group 4 – Zn-Ni-Co Plating with various current densities

In the first three experimental groups, after using single and double surfaces, coatings were made with different thicknesses. Thereupon, for the last experimental group, the Zn-Ni-Co alloy, which has superior efficiency among all coatings, was examined through the data statistics table in addition to the graphs, and coated on the substrate. Sample selection was made by giving priority to the one with high shielding efficiency.

Table 7.4 Data statistics table of Group 1, 2 and 3 for comparing EMI-SE

Data evaluation priority : mean > max = min > standard deviation = range		Alloy Coatings				
		Cu	**Zn-Ni**	**Zn-Co**	**Ni-Co**	**Zn-Ni-Co**
Group 1 – One-Sided Plating	**min**	-39.57	-82.98	-77.82	-77.99	-84.30
	mean	-37.62	-76.27	-65.32	-75.98	-78.48
	max	-36.18	-64.88	-46.11	-69.19	-72.50
	range	3.39	18.10	31.72	8.80	11.80
	std deviation	1.32	6.09	11.25	0.94	2.07
Group 2 – Two-Sided Plating	**min**	-84.47	-83.77	-80.04	-82.87	-79.70
	mean	-78.23	-75.21	-73.64	-77.68	-70.63
	max	-69.29	-68.68	-57.29	-71.71	-55.53
	range	15.18	15.09	22.75	11.16	24.17
	std deviation	2.00	3.89	5.35	3.56	6.14
Group 3 – Two-Sided Thick Plating	**min**	-85.16	-91.30	-82.77	-83.87	-82.41
	mean	-78.42	-78.39	-79.53	-77.62	-79.23
	max	-74.12	-75.22	-73.55	-71.93	-74.80
	range	11.04	16.08	9.22	11.94	7.60
	std deviation	2.52	2.25	2.11	2.87	2.35

Table 7.5 Data statistics table of Group 1, 2 and 3 for comparing absorption

Data evaluation priority : mean > max = min > standard deviation = range		Alloy Coatings				
		Cu	**Zn-Ni**	**Zn-Co**	**Ni-Co**	**Zn-Ni-Co**
Group 1 – One-Sided Plating	**min**	-0.233	-0.667	-0.152	-0.472	-0.493
	mean	-0.090	-0.138	-0.039	-0.316	-0.104
	max	-0.045	-0.085	0.104	-0.059	0.570
	range	0.278	0.752	0.256	0.413	0.549
	std deviation	0.071	0.172	0.070	0.109	0.129
Group 2 – Two-Sided Plating	**min**	very similar to Group 1				
	mean					
	max					
	range					
	std deviation					
Group 3 – Two-Sided Thick Plating	**min**	-0.314	-0.804	-0.371	-0.291	-0.522
	mean	-0.057	-0.129	-0.105	-0.053	-0.116
	max	0.115	0.114	0.111	0.138	0.035
	range	0.429	0.918	0.482	0.429	0.557
	std deviation	0.079	0.19	0.115	0.1	0.099

For the group 4 experiments, four different current values were initially selected as I = 0.25 A, I = 0.5 A, I = 1 A and I = 2 A, each time with current densities twice the previous one. Later, the I = 0.75 A value was added with the fifth sample in order to diversify.

7.4.1 Characterization of Zn-Ni-Co coatings

The surface of the copper sample immersed in 250 mL electrolyte for Zn-Ni-Co coating, which is in contact with the electrolyte, has an area of 30 x 40 mm (0.12 dm^2). While different current density studies were carried out, different current values were applied to each sample (Table 7.6). The current density results corresponding to these current values were also calculated and then the coating thicknesses were also measured and added to Table 7.6.

Table 7.6 Current density values depending on the applied current - thickness of Zn-Ni-Co coatings

	Zn-Ni-Co coating				
Applied Current (A)	0.25	0.5	1	2	0.75
Current density (A/dm^2)	2.08	4.17	8.33	16.67	6.25
Coating thickness (μm)	6.4 ± 1.47	10.8 ± 1.60	14.1 ± 2.90	21.7 ± 2.73	12.3 ± 2.09

7.4.1.1 SEM examination

The surface morphologies of Zn-Ni-Co alloy coatings coated on copper substrate with different current densities by electrolytic method are given in Figure 7.18. The network-like indented-eaved surface morphology that started at low current density (Figure 7.18 a, b, c, d) became more pronounced at medium current density and a leaf-like structure began to form (Figure 7.18 e, f). At high current density, the surfaces exhibited changes as more compact and less leafy surfaces (Figure 7.18 g, h). When the current density exceeded a certain value, deterioration, cracks and fractures were observed in the coating structure (Figure 7.18 i, j). The reason for these is that the sudden high current cannot form the coating equally in every area and the integrity of the structure cannot be maintained. As shown in Table 7.7, the Zn-Ni-Co coating layers produced at varying current densities contain an average of 68.4 % Zn, 7.22 % Ni and 2.88 % Co. One of the factors affecting this change in morphology is the change in the Ni and Co ratios.

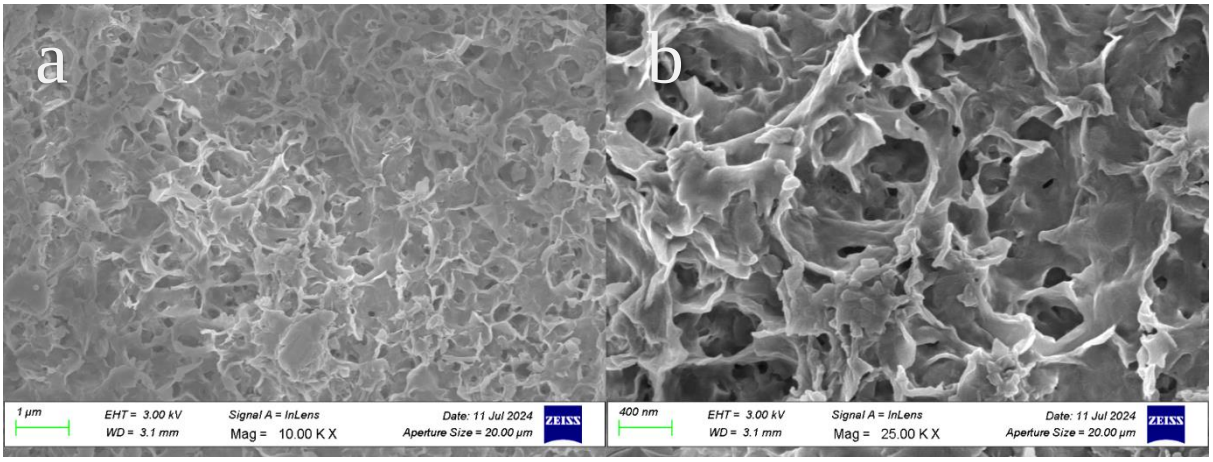
a
b
1 µm
EHT = 3.00 kV
WD = 3.1 mm
Signal A = InLens
Mag = 10.00 K X
Date: 11 Jul 2024
Aperture Size = 20.00 µm
ZEISS
400 nm
EHT = 3.00 kV
WD = 3.1 mm
Signal A = InLens
Mag = 25.00 K X
Date: 11 Jul 2024
Aperture Size = 20.00 µm
ZEISS

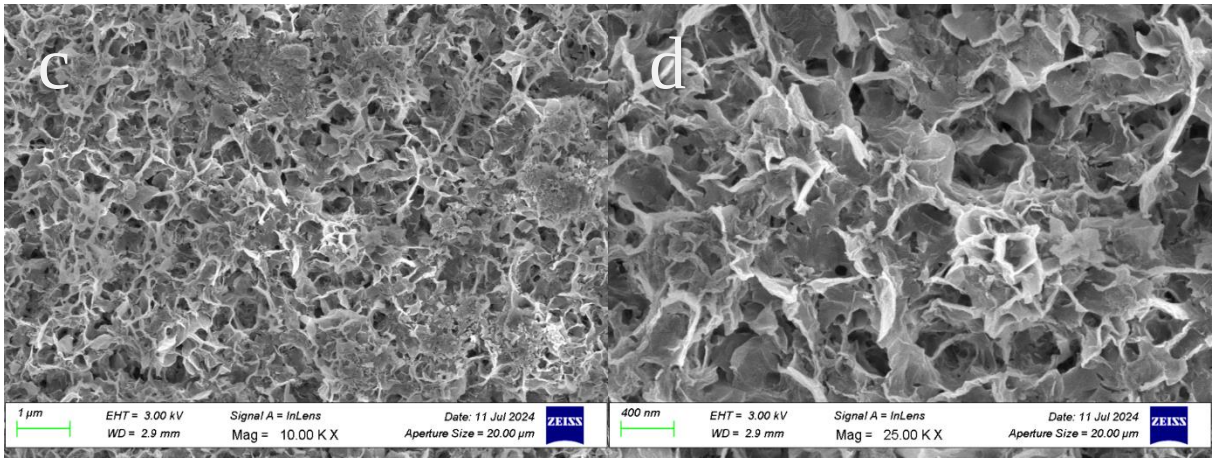
c
d
1 µm
EHT = 3.00 kV
WD = 2.9 mm
Signal A = InLens
Mag = 10.00 K X
Date: 11 Jul 2024
Aperture Size = 20.00 µm
ZEISS
400 nm
EHT = 3.00 kV
WD = 2.9 mm
Signal A = InLens
Mag = 25.00 K X
Date: 11 Jul 2024
Aperture Size = 20.00 µm
ZEISS

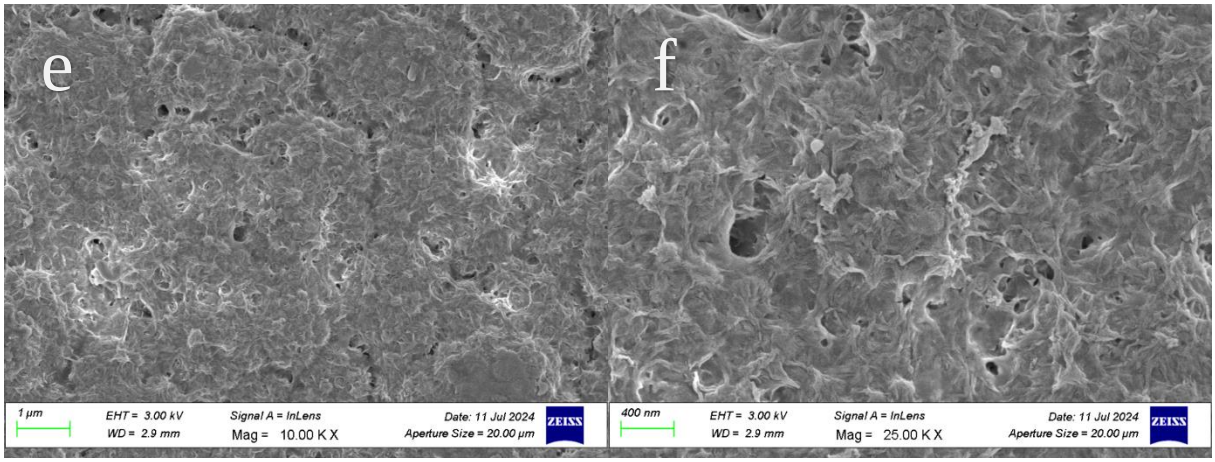
e
f
1 µm
EHT = 3.00 kV
WD = 2.9 mm
Signal A = InLens
Mag = 10.00 K X
Date: 11 Jul 2024
Aperture Size = 20.00 µm
ZEISS
400 nm
EHT = 3.00 kV
WD = 2.9 mm
Signal A = InLens
Mag = 25.00 K X
Date: 11 Jul 2024
Aperture Size = 20.00 µm
ZEISS

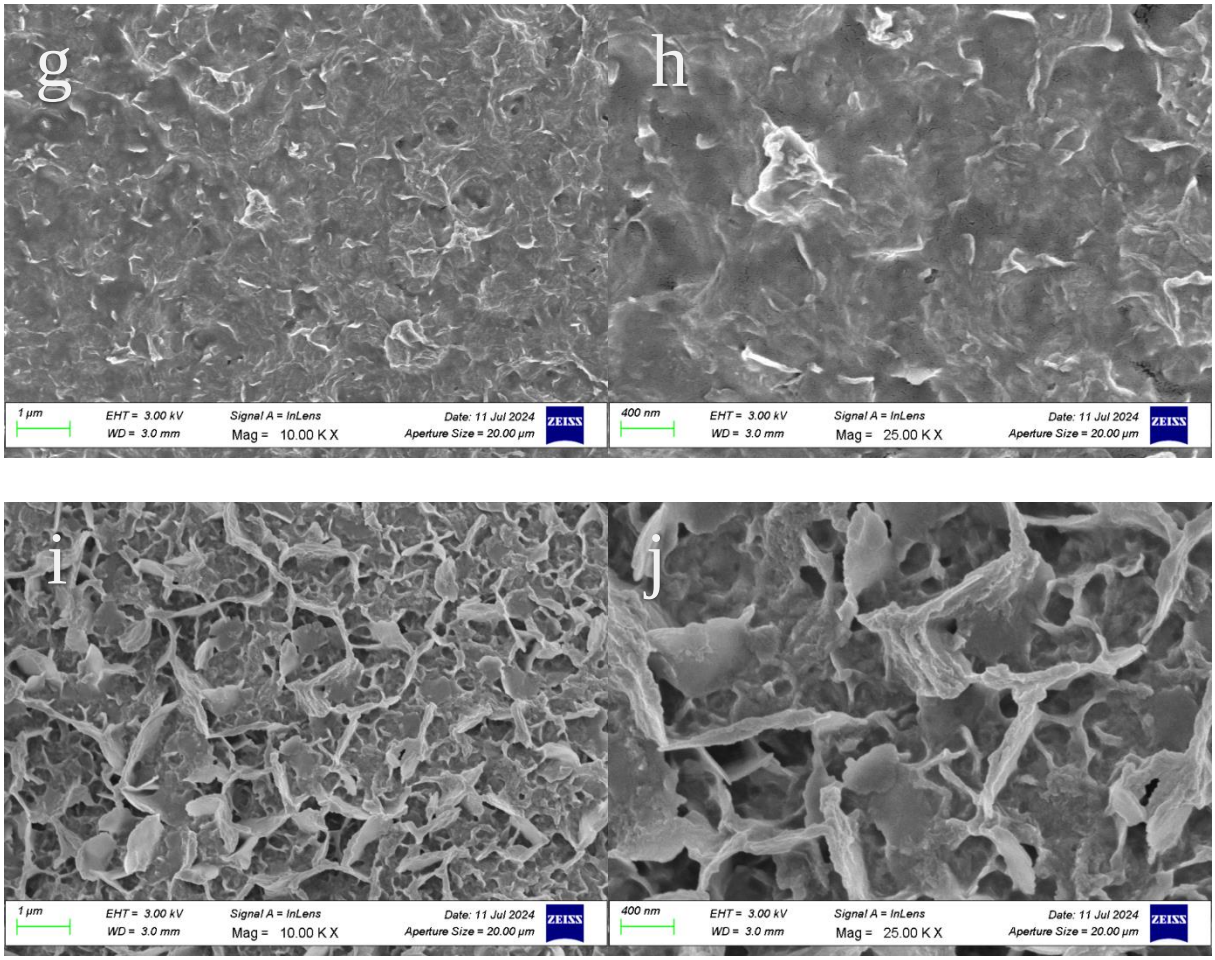

Figure 7.18 SEM images of Zn-Ni-Co alloy coated at (a, b) I = 0.25 A, (c, d) I = 0.5 A, (e, f) I = 0.75 A , (g, h) I = 1 A and (i, j) I = 2 A

Table 7.7 The EDS results of Zn-Ni-Co alloy coatings at various current values

	Zn-Ni-Co (I = 0.25 A) (%)	**Zn-Ni-Co (I = 0.5 A) (%)**	**Zn-Ni-Co (I = 0.75 A) (%)**	**Zn-Ni-Co (I = 1 A) (%)**	**Zn-Ni-Co (I = 2 A) (%)**
Zn	69.8	73.9	68.9	70.4	59.0
Ni	6.2	6.7	8.1	8.7	6.4
Co	1.5	1.4	3.4	2.5	5.6
Others	22.5	18.0	19.6	18.4	29.0

7.4.1.2 XRD studies

Figure 7.19 displays the XRD patterns of the Zn-Ni-Co alloy coating on the copper tape at different current densities. The maximum peak at 2θ=50.4° in each sample corresponds to the substrate. Given that the Co wt% in the coating at I = 0.25 A is as low as in group 1, the three reflections at 2θ=36.28°, 2θ=38.92°, and 2θ=43.28° confirm this phenomenon. In sample where I = 0.5 A, the peaks are similar to I = 0.25 A sample but stronger, showing the importance of current density. The peak at 54.2° also proves this point. In I = 0.75 A sample, a transition graph is seen to the phase distribution at upper current densities, where the Ni_5Zn_{21} peak starts to disappear and the pure Zn peaks also gradually disappear. In samples where I = 1 A and I = 2 A, the Ni_5Zn_{21} peak and some pure Zn peaks did not occur and a completely different phase distribution was observed. In sample I = 2 A, the 2θ=50.4° peak coming from the substrate seems a little weaker than normal, but it is still present.

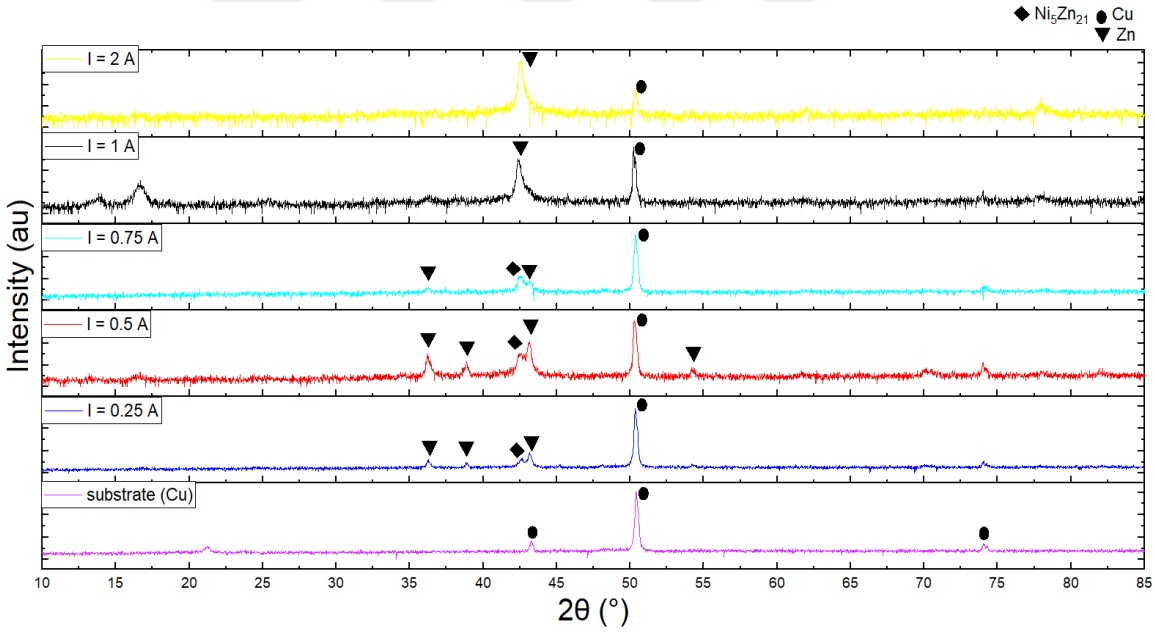

Figure 7.19 XRD patterns of Zn-Ni-Co coatings produced at varying current values

7.4.2 VNA studies

The results obtained from three experimental groups, in which first the number of coated surfaces and then the coating time and thus the coating thickness were changed,

were evaluated, provided that other parameters were kept the same. Zn-Ni-Co coating was chosen as the sample with the peak shielding and absorption efficiency. In the current section, the electromagnetic interference (EMI) shielding and absorption performances of the preferred Zn-Ni-Co coating at diverse current densities were examined.

7.4.2.1 EMI-SE examination

Figure 7.20 shows the S parameters data of Zn-Ni-Co samples studied at various current densities. Compared to the substrate, all samples demonstrated improved efficiency in every part of the X-band (except for the 9.6 – 10.2 GHz frequency range results for the sample with I = 0.25 A).

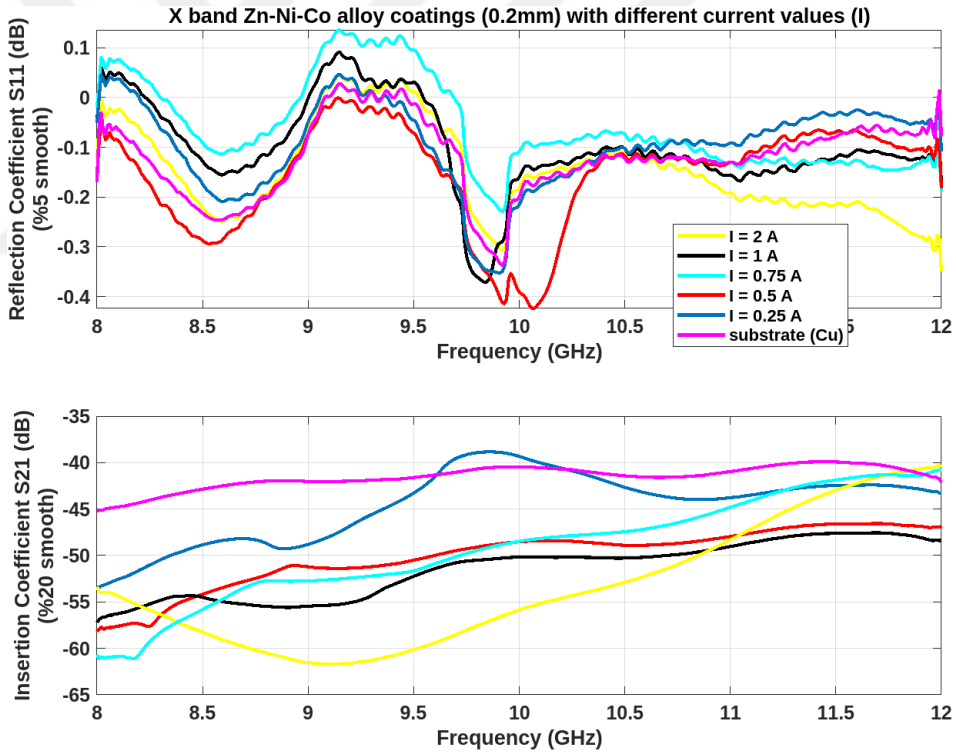

Figure 7.20 Reflection (S11) – insertion (S21) data of platings and substrate (copper foil tape) (Group-4)

As in each experimental group, Eq. (1) was used in the SE calculation. All materials performed well on the substrate and were within the shielding efficiency range considered good. Since they are made of the same material and their styles are similar,

a wavy graph has emerged as seen in Figure 7.21. Although sample I = 2 A has a higher shielding value compared to the others between frequencies 8.4-10.8 GHz, it appears to have a lower value in the range of 8-8.5 GHz, where almost all of them are in good condition. After using the graph and Table 7.8 together, it was understood that the I = 0.25 A sample should not be preferred too much, and that the I = 1 A sample, although it lags behind I = 2 A sample in a certain range, was the product that gave the best yield because it was generally the most stable. That is because thee significant problems (deformation, cracks, insufficient formation of characteristic peaks) of the sample produced at I = 2 A, which appeared in other analyzes, did not make it possible to consider it as a sample with good results. Another point to note is that the I = 0.5 A sample produced in the previous experimental groups has an efficiency very close to I = 1 A sample.

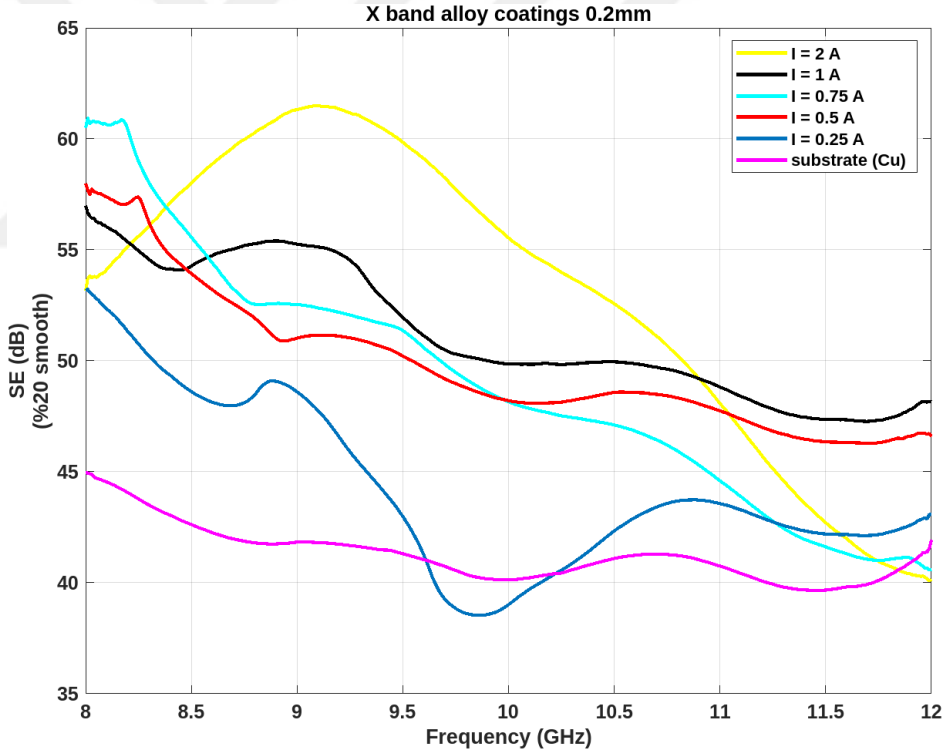

Figure 7.21 SE (dB) data of platings (Group-4)

Table 7.8 Data stats table of Group 4 for comparing EMI-SE

Data evaluation priority : mean > max = min > standard deviation = range		Zn-Ni-Co Alloy Coatings					
		I = 0.25 A	**I = 0.5 A**	**I = 0.75 A**	**I = 1 A**	**I = 2 A**	**Substrate (Cu)**
Group 4 – Zn-Ni-Co Plating with various current values	**min**	-53.98	-58.19	-61.25	-59.19	-62.46	-45.17
	mean	-44.45	-50.01	-49.12	-51.41	-53.49	-41.46
	max	-37.38	-46.22	-40.79	-47.20	-40.29	-39.35
	range	16.60	11.98	20.46	11.99	22.16	5.82
	std deviation	4.38	3.29	5.60	3.24	6.91	1.35

7.4.2.2 Absorbance

When the change from Figure 7.22 (a) to (b) is examined, in 7.22 (b) the I = 2 A sample is the sample that gives the best efficiency along the X-band, except that the I = 1 A sample showed better performance in the 9.6-9.8 GHz range. However, as mentioned in the general shielding section, when the I = 2 A sample is excluded from the evaluation, the best efficiency is still obtained from the I = 1 A sample.

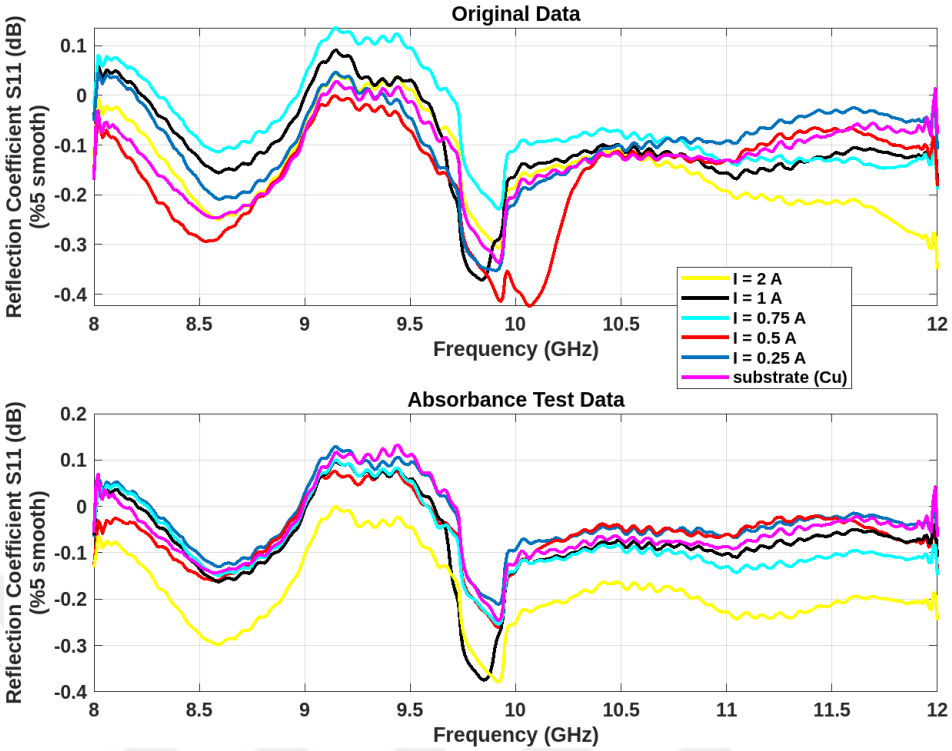

Figure 7.22 Absorbance (S11) values of platings and substrate material (a) original, (b) after absorbance testing (Group-4)

CHAPTER EIGHT
CONCLUSIONS AND FUTURE WORK

In this study, Zn-Ni, Zn-Co, Ni-Co and Zn-Ni-Co metal alloy coatings were manufactured by electroplating method and their electromagnetic interference shielding, and absorption properties were investigated. Current density, coating time, and double-surface coating were selected as the variables, except for special specifications.

Initially, shielding performances were measured with alloy coating applications applied to a single surface. Then, alloy coatings were applied to the double surface of copper to determine whether they gave better efficiency than the initial state. In the next experimental group, a thicker coating was formed by increasing the coating time and the electromagnetic interference shielding & absorption behaviors of these new samples were investigated. When all data were examined, an average of 78.48 and 79.23 dB was obtained for shielding property for Zn-Ni-Co, Groups 1 and 3, respectively; and an average of 0.316 dB was obtained for absorption property for Ni-Co, Groups 1 and 2, respectively. The alloy coating Zn-Ni-Co, which gave the best results in the process (with shielding as a priority), was selected and the effect of current density was investigated in subsequent experiments.

A total of 4 groups of experiments were performed. Variable surface structures and morphologies of alloy coatings were obtained. The elemental change in the alloy type is the most important factor. Both shielding and absorption values were improved at each stage. The differences in the latter data from the former are not significant as the data for each group are within the specified limits. More significant increases were obtained in the electromagnetic shielding section compared to absorption values.

In the experimental group where the current density was studied, it was observed that the samples prepared at the current values of I = 0.5 A used in previous experiments and I = 1 A only in this group were close to each other and showed the best efficiency. Since current density is the most essential factor affecting the

properties of the coating, the role of this variable was investigated on the Zn-Ni-Co coating type, which showed the best shielding performance among four different alloy types. This does not change the fact that other factors are also significant.

For similar studies to be conducted in the future, variables such as coating time (in a wider scale), coating thickness, and pH of the electrolyte can be used. Further results can be observed with the same parameters under the main headings of single-sided and double-sided coatings. By combining two different sample properties that show high shielding performance, a different and better result can be obtained. This study sheds light on new studies that other different pure and alloyed coating types can also be used for shielding performance.

REFERENCES

Aliofkhazraei, M., Walsh, F. C., Zangari, G., Köçkar, H., Alper, M., Rizal, C., ... & Allahyarzadeh, M. H. (2021). Development of electrodeposited multilayer coatings: A review of fabrication, microstructure, properties and applications. *Applied Surface Science Advances*, *6*, 100141.

Araz, I. (2018). The measurement of shielding effectiveness for small-in-size ferrite-based flat materials. *Turkish Journal of Electrical Engineering and Computer Sciences*, *26*(6), 2996-3006.

Ashassi-Sorkhabi, H., & Rafizadeh, S. H. (2004). Effect of coating time and heat treatment on structures and corrosion characteristics of electroless Ni–P alloy deposits. *Surface and coatings Technology*, *176*(3), 318-326.

Bhat, R. S., & Shet, V. B. (2020). Development and characterization of Zn–Ni, Zn–Co and Zn–Ni–Co coatings. *Surface Engineering*, *36*(4), 429-437.

Bheema, R. K., & Etika, K. C. (2023). The influence of hybrid decorated structures on the EMI shielding properties of epoxy composites over the X-Band. *Materials Today: Proceedings*, *76*, 398-402.

BRENNER, A. (1963). Electrodeposition of Alloys. *Principle and Practice*, 1-615.

Chen, H., Zhang, Q., Han, X., Cai, J., Liu, M., Yang, Y., & Zhang, K. (2015). 3D hierarchically porous zinc–nickel–cobalt oxide nanosheets grown on Ni foam as binder-free electrodes for electrochemical energy storage. *Journal of Materials Chemistry A*, *3*(47), 24022-24032.

Creighton, J. R., & Ho, P. (2001). Introduction to chemical vapor deposition (CVD). *Chemical vapor deposition*, *2*, 1-22.

CRESPO RIBADENEYRA, Maria. *EMI SHIELDING COMPOSITES BASED ON MAGNETIC NANOPARTICLES AND NANOCARBONS*. Doctoral Thesis, Universidad Carlos III de Madrid, 2014

Croll, S. G. (2020). Surface roughness profile and its effect on coating adhesion and corrosion protection: A review. *Progress in organic coatings*, *148*, 105847.

ÇETİNKAYA, Efdal. *ÇİNKO-NİKEL ALAŞIM KAPLAMALARININ KARAKTERİSTİKLERİNİN İNCELENMESİ.* Yüksek Lisans Tezi, Yıldız Teknik Üniversitesi, 2006

de Carli, T. (2022). Optimization of barrel electroplating process for acid zinc.

Devaraj, G., Guruviah, S., & Seshadri, S. K. (1990). Pulse plating. *Materials Chemistry and physics*, *25*(5), 439-461.

Di Bari, G. A. (2010). Modern Electroplating Chapter 3: Electrodeposition of Nickel, ; Schlesinger, M., Paunovic, M.

DİKİCİ, Tuncay. *ÇELİK MALZEME YÜZEYİNE ELEKTROLİTİK YOLLA KAPLANAN ZN-Nİ-CO ALAŞIMININ MEKANİK VE YAPISAL ÖZELLİKLERİNİN İNCELENMESİ.* Yüksek Lisans Tezi, Dokuz Eylül Üniversitesi, 2009

Durán, A., Castro, Y. A., Aparicio, M., Conde, A., & De Damborenea, J. J. (2007). Protection and surface modification of metals with sol–gel coatings. *International materials reviews*, *52*(3), 175-192.

Eliaz, N., Venkatakrishna, K., & Hegde, A. C. (2010). Electroplating and characterization of Zn–Ni, Zn–Co and Zn–Ni–Co alloys. *Surface and coatings technology*, *205*(7), 1969-1978.

Elkhatabi, F., Benballa, M., Sarret, M., & Müller, C. (1999). Dependence of coating characteristics on deposition potential for electrodeposited Zn–Ni alloys. *Electrochimica Acta*, *44*(10), 1645-1653.

Fotovvati, B., Namdari, N., & Dehghanghadikolaei, A. (2019). On coating techniques for surface protection: A review. *Journal of Manufacturing and Materials processing*, *3*(1), 28.

FRAHM, Matthew Ryan. *ELECTROMAGNETIC INTERFERENCE SHIELDING EFFECTIVENESS OF COMPOSITE MATERIALS*. Master's Thesis, North Carolina State University, 2013

Geetha, S., Satheesh Kumar, K. K., Rao, C. R., Vijayan, M., & Trivedi, D. C. (2009). EMI shielding: Methods and materials—A review. *Journal of applied polymer science*, *112*(4), 2073-2086.

Ghaziof, S., & Gao, W. (2014). Electrodeposition of single gamma phased Zn–Ni alloy coatings from additive-free acidic bath. *Applied Surface Science*, *311*, 635-642.

Gill, B. J., & Tucker, R. C. (1986). Plasma spray coating processes. *Materials science and technology*, *2*(3), 207-213.

GÜNEY, İbrahim. *ELEKTRO KAPLAMA YÖNTEMİYLE PASLANMAZ ÇELİK ÜZERİNE RH VE AG FİLM KAPLAMALARIN KOROZYON ÖZELLİKLERİNİN ARAŞTIRILMASI.* Yüksek Lisans Tezi, Atatürk Üniversitesi, 2020

HASÇALIK, A., & Özek, C. (2002). Elektroliz Yöntemiyle Çinko Kaplama Parametrelerinin İncelenmesi. *JESTECH (Engineering Sci. Technol*, *1*, 2.

Hulse, D. (1993). Electrolytes and their properties. *Transactions of the IMF*, *71*(1), 41-43.

Iqbal, A., Hassan, T., Gao, Z., Shahzad, F., & Koo, C. M. (2023). MXene-incorporated 1D/2D nano-carbons for electromagnetic shielding: A review. *Carbon*, *203*, 542-560.

İRGİN, Dilara. *NİKEL ELEKTRO KAPLAMANIN KARBON FİBERİN ELEKTROMANYETİK GİRİŞİM KALKANLAMA ÖZELLİĞİNE ETKİSİ.* Yüksek Lisans Tezi, Başkent Üniversitesi, 2022

Jiang, J., Liu, X. X., Han, J., Hu, K., & Chen, J. S. (2021). Self-supported sheets-on-wire CuO@ Ni (OH) 2/Zn (OH) 2 nanoarrays for high-performance flexible quasi-solid-state supercapacitor. *Processes*, *9*(4), 680.

Kalantary, M. R. (1994). Zinc alloy electrodeposition for corrosion protection. *Plating and surface finishing*, *81*(6), 80-88.

Kanani, N. (2004). *Electroplating: basic principles, processes and practice*. Elsevier.

Karahan, I. H., Karabulut, O., & Alver, U. (2009). A study on electrodeposited Zn–Co alloys. *Physica Scripta*, *79*(5), 055801.

Karimzadeh, A., Aliofkhazraei, M., & Walsh, F. C. (2019). A review of electrodeposited Ni-Co alloy and composite coatings: Microstructure, properties and applications. *Surface and Coatings Technology*, *372*, 463-498.

KAVAK, Salim. *SERT KROM KAPLAMADA İŞLEM PARAMETRELERİNİN KAPLAMA ÜZERİNE ETKİLERİNİN ARAŞTIRILMASI.* Yüksek Lisans Tezi, Gazi Üniversitesi, 2001

Kim, J. J., Lee, H. W., Dabhade, V. V., Kim, S. R., Kwon, W. T., Choi, D. J., ... & Kim, Y. (2010). Electro magnetic interference shielding characteristic of silver coated copper powder. *Metals and Materials International*, *16*, 469-475.

Koehler, W.A., (1944), "Principles and Applications of Electrochemistry", *John Wiley and Sons Inc.*

Kumar, A., & Singh, S. (2018, March). Development of coatings for radar absorbing materials at X-band. In *IOP Conference Series: Materials Science and Engineering* (Vol. 330, No. 1, p. 012006). IOP Publishing.

Li, J. Y., Ni, C., Liu, J. Y., Jin, M. J., Li, W., & Jin, X. J. (2014). Extraordinary stability of nano-twinned structure formed during phase transformation coupled with grain growth in electrodeposited Co–Ni alloys. *Materials Chemistry and Physics*, *148*(3), 1202-1211.

Li, Y. T., & Sun, Y. T. A. (2022). An investigation of electromagnetic interference shielding effectiveness with multilayer thin films material. *Thin Solid Films*, *753*, 139259.

Lima-Neto, D., Correia, A. N., Colares, R. P., & Araujo, W. S. (2007). Corrosion study of electrodeposited Zn and Zn-Co coatings in chloride medium. *Journal of the Brazilian Chemical Society*, *18*, 1164-1175.

Liu, H., Li, J., & Wang, L. (2010). Electroless nickel plating on APTHS modified wood veneer for EMI shielding. *Applied Surface Science*, *257*(4), 1325-1330.

Lodhi, Z. F., Tichelaar, F. D., Kwakernaak, C., Mol, J. M. C., Terryn, H., & De Wit, J. H. W. (2008). A combined composition and morphology study of electrodeposited Zn–Co and Zn–Co–Fe alloy coatings. *Surface and Coatings Technology*, *202*(12), 2755-2764.

Lupi, C., Dell'Era, A., Pasquali, M., & Imperatori, P. (2011). Composition, morphology, structural aspects and electrochemical properties of Ni–Co alloy coatings. *Surface and Coatings Technology*, *205*(23-24), 5394-5399.

Mahieu, J., De Wit, K., De Cooman, B. C., & De Boeck, A. (1999). The properties of electrodeposited Zn-Co coatings. *Journal of materials engineering and performance*, *8*, 561-570.

Mallory, G. O., & Hajdu, J. B. (Eds.). (1990). *Electroless plating: fundamentals and applications*. William Andrew.

MANAZOĞLU, Mert. *ELEKTROKİMYASAL YÖNTEMLE NİKEL MOLİBDEN ALAŞIM KAPLAMALARIN ÜRETİMİ VE KARAKTERİZASYONU.* Yüksek Lisans Tezi, Dokuz Eylül Üniversitesi, 2013

Mattox, D. M. (2010). *Handbook of physical vapor deposition (PVD) processing*. William Andrew.

Mishra, R. K., Thomas, M. G., Abraham, J., Joseph, K., & Thomas, S. (2018). Electromagnetic interference shielding materials for aerospace application: A state of the art. *Advanced Materials for Electromagnetic Shielding: Fundamentals, Properties, and Applications*, 327-365.

Nasirpouri, F., Alipour, K., Daneshvar, F., & Sanaeian, M. R. (2020). Electrodeposition of anticorrosion nanocoatings. In *Corrosion Protection at the Nanoscale* (pp. 473-497). Elsevier.

Nazeer, A. A., & Madkour, M. (2018). Potential use of smart coatings for corrosion protection of metals and alloys: A review. *Journal of Molecular Liquids*, *253*, 11-22.

Ohno, I. (1991). Electrochemistry of electroless plating. *Materials Science and Engineering: A*, *146*(1-2), 33-49.

Panek, J., Bierska-Piech, B., Łągiewka, E., & Budniok, A. (2010). Electrodeposition and the properties of composite Zn+ Ni coatings. *Surface and Interface Analysis*, *42*(6-7), 1226-1230.

Qing, Y., Yao, H., Li, Y., & Luo, F. (2021). Plasma-sprayed ZrB2/Al2O3 ceramics with excellent high temperature electromagnetic interference shielding properties. *Journal of the European Ceramic Society*, *41*(2), 1071-1075.

Rahman, M. J., Sen, S. R., Moniruzzaman, M., & Shorowordi, K. M. (2009). Morphology and properties of electrodeposited Zn-Ni alloy coatings on mild steel. *Journal of Mechanical Engineering*, *40*(1), 9-14.

Ramírez, C., Shamshirgar, A. S., Pérez-Coll, D., Osendi, M. I., Miranzo, P., Tewari, G. C., ... & Belmonte, M. (2023). CVD nanocrystalline multilayer graphene coated 3D-printed alumina lattices. *Carbon*, *202*, 36-46.

Rose, I., & Whittington, C. (2022). *Nickel Plating Handbook* (William, L. W. Ed.). Nickel Institute. (Original work published 2014)

SAVAŞ, Eren. *ELEKTROMANYETİK KALKANLAMA UYGULAMALARI İÇİN POLİMERİK KOMPOZİT FİLMLERİN SENTEZLENMESİ*. Yüksek Lisans Tezi, Ankara Hacı Bayram Veli Üniversitesi, 2023

Sekar, R., Jagadesh, K. K., & Bapu, G. R. (2015). Development of black Ni–Co alloy films from modified Watts electrolyte and its morphology and structural characteristics. *Transactions of Nonferrous Metals Society of China*, *25*(6), 1961-1967.

Shirke, N., Ghase, V., & Jamdar, V. (2024). Recent advances in stealth coating. *Polymer Bulletin*, 1-30.

Soderberg, G., Pinner, W. L., & Baker, E. M. (1941). Cobalt Plating. *Transactions of The Electrochemical Society*, *80*(1), 579.

Sparks, J. (2008). The basics of alkaline in-process cleaning for metal substrates. *Oakite Products, Inc*, *8*.

Sriraman, K. R., Brahimi, S., Szpunar, J. A., Osborne, J. H., & Yue, S. (2013). Characterization of corrosion resistance of electrodeposited Zn–Ni Zn and Cd coatings. *Electrochimica Acta*, *105*, 314-323.

Sun, L., Yuan, G., Gao, L., Yang, J., Chhowalla, M., Gharahcheshmeh, M. H., ... & Liu, Z. (2021). Chemical vapour deposition. *Nature Reviews Methods Primers*, *1*(1), 5.

Suryanarayanan, R. (1993). *Plasma spraying: theory and applications*. World scientific.

Tian, L., Xu, J., & Xiao, S. (2011). The influence of pH and bath composition on the properties of Ni–Co coatings synthesized by electrodeposition. *Vacuum*, *86*(1), 27-33.

Tóth, B. G., Péter, L., Dégi, J., Révész, Á., Oszetzky, D., Molnár, G., & Bakonyi, I. (2013). Influence of Cu deposition potential on the giant magnetoresistance and surface roughness of electrodeposited Ni–Co/Cu multilayers. *Electrochimica Acta*, *91*, 122-129.

Tozar, A., & Karahan, I. H. (2014). Structural and corrosion protection properties of electrochemically deposited nano-sized Zn–Ni alloy coatings. *Applied Surface Science*, *318*, 15-23.

Tushinsky, L. (2002). *Coated metal: structure and properties of metal-coating compositions*. Springer Science & Business Media.

Wang, J., Gabe, D. R., Hart, A. C., & Crouch, P. C. (2013). The chemistry of nickel electroplating solutions. *Transactions of the IMF*, *91*(1), 4-10.

Wu, L. K., Wu, J. J., Wu, W. Y., Cao, F. H., & Jiang, M. Y. (2020). Sol–gel-based coatings for oxidation protection of TiAl alloys. *Journal of materials science*, *55*, 6330-6351.

Yahalom, J., & Zadok, O. (1987). Formation of composition-modulated alloys by electrodeposition. *Journal of materials science*, *22*, 499-503.

Yang, Y. F., Deng, B., & Wen, Z. H. (2011). Preparation of Ni-Co alloy foils by electrodeposition. *Advances in Chemical engineering and science*, *1*(2), 27-32.

Ye, W., Fu, J., Wang, Q., Wang, C., & Xue, D. (2015). Electromagnetic wave absorption properties of NiCoP alloy nanoparticles decorated on reduced graphene oxide nanosheets. *Journal of Magnetism and Magnetic Materials*, *395*, 147-151.

Zamani, M., Amadeh, A., & Baghal, S. L. (2016). Effect of Co content on electrodeposition mechanism and mechanical properties of electrodeposited Ni–Co alloy. *Transactions of Nonferrous Metals Society of China*, *26*(2), 484-491.

Zeng, Z., Wu, T., Han, D., Ren, Q., Siqueira, G., & Nyström, G. (2020). Ultralight, flexible, and biomimetic nanocellulose/silver nanowire aerogels for electromagnetic interference shielding. *Acs Nano*, *14*(3), 2927-2938.

Zhang, W., Du, S., Li, B., Mei, T., Miao, Y., Chu, H., & Wang, J. (2021). Synthesis and characterization of TiN nanoparticle reinforced binary Ni-Co alloy coatings. *Journal of Alloys and Compounds*, *865*, 158722.